

ALTERNATING MINIMIZATION ALGORITHMS FOR GRAPH REGULARIZED TENSOR COMPLETION

YU GUAN*, SHUYU DONG[†], BIN GAO[‡], P.-A. ABSIL[§], AND FRANÇOIS GLINEUR[¶]

Abstract. We consider a Canonical Polyadic (CP) decomposition approach to low-rank tensor completion (LRTC) by incorporating external pairwise similarity relations through graph Laplacian regularization on the CP factor matrices. The usage of graph regularization entails benefits in the learning accuracy of LRTC, but at the same time, induces coupling graph Laplacian terms that hinder the optimization of the tensor completion model. In order to solve graph-regularized LRTC, we propose efficient alternating minimization algorithms by leveraging the block structure of the underlying CP decomposition-based model. For the subproblems of alternating minimization, a linear conjugate gradient subroutine is specifically adapted to graph-regularized LRTC. Alternatively, we circumvent the complicating coupling effects of graph Laplacian terms by using an alternating directions method of multipliers. Based on the Kurdyka-Łojasiewicz property, we show that the sequence generated by the proposed algorithms globally converges to a critical point of the objective function. Moreover, the complexity and convergence rate are also derived. In addition, numerical experiments including synthetic data and real data show that the graph regularized tensor completion model has improved recovery results compared to those without graph regularization, and that the proposed algorithms achieve gains in time efficiency over existing algorithms.

Key words. Tensor completion, graph Laplacian regularization, alternating minimization, alternating direction method of multiplier, Kurdyka-Łojasiewicz property

AMS subject classifications. 15A69, 49M20, 65B05, 90C26, 90C30, 90C52

1. Introduction. Matrix and tensor (also known as multidimensional arrays) completion arise in many areas such as signal processing for EEG data [37] and MRI (magnetic resonance imaging) [5], genetic data analysis [31] and image and video restoration [8, 33]. In these applications, the data matrix or data tensor is often only partially observed, undersampled, or sampled with noise; matrix or tensor completion is an abstraction of the problem of recovering such data. While it is unlikely to recover the missing data if the hidden matrix or tensor is unstructured, it is shown that matrix completion can indeed be solved when the hidden matrix has a low rank [11, 44], and instead of the matrix rank, the matrix nuclear norm is a convex relaxation that guarantees exact solutions to the low-rank matrix completion problem [35]. Generalizing from the matrix case to the tensor case, several works [20, 33] extended the matrix nuclear norm-based regularization to the tensor completion problem. Liu et al. [32] introduced an extension of the matrix nuclear norm to the low-rank tensor completion (LRTC) problem and later defined the nuclear norm of a tensor as a convex combination of nuclear norms of its unfolding matrices [33]. Given an k -th order tensor $\mathcal{T} \in \mathbb{R}^{m_1 \times \dots \times m_k}$, the nuclear norm-based tensor completion model is as follows,

$$\min_{\mathcal{Z} \in \mathbb{R}^{m_1 \times \dots \times m_k}} \frac{1}{2} \|\mathcal{P}_\Omega(\mathcal{T} - \mathcal{Z})\|_{\text{F}}^2 + \sum_{i=1}^k \lambda_i \|\mathcal{Z}_{(i)}\|_*, \quad (1.1)$$

where \mathcal{P}_Ω is the projection operator that only retains the revealed entries of \mathcal{T} , recorded in the index set $\Omega \subset [m_1] \times \dots \times [m_k]$, and $\|\mathcal{Z}_{(i)}\|_*$ denotes the matrix nuclear norm of the mode- i matricization (Section 2) of \mathcal{Z} . The nuclear norm terms $\|\mathcal{Z}_{(i)}\|_*$ in (1.1) promote solutions of \mathcal{Z} with low-rank matricizations. However, the model (1.1) has a memory requirement of $O(m_1 \dots m_k)$, and the nuclear norm term in (1.1) involves subdifferential computations that require singular value decomposition of the unfolding matrices $\mathcal{Z}_{(i)}$, which can be very large since their sizes ($m_i \times \prod_{j \neq i} m_j$) grow quickly with the tensor size (m_1, \dots, m_k) . Therefore, many LRTC approaches use low-rank tensor decompositions such as the Tucker decomposition and the Canonical Polyadic (CP) decomposition to systematically limit the number of parameters of the tensor

*Huawei European Research Institute (ricky7guanyu@gmail.com)

[†]LISN, INRIA, Université Paris-Saclay (shuyu.dong@inria.fr)

[‡]LSEC, Academy of Mathematics and Systems Science, Chinese Academy of Sciences (gaobin@lsec.ac.cn)

[§]Department of INMA, Université catholique de Louvain (pa.absil@uclouvain.be)

[¶]Department of INMA, Université catholique de Louvain (francois.glineur@uclouvain.be)

model [25, 55, 39, 29, 19]. Other decomposition-based approaches to the LRTC problem include hierarchical tensor representations [17, 43], tensor train decomposition [49, 10] and tensor ring decomposition [51, 21].

In addition to low-rankness, auxiliary similarity information about the inter-relations between data entries, also called side information, is also an important source for refining the solutions of data recovery problems such as matrix and tensor completion. For matrix completion, auxiliary information is used in the form of graph regularization [48, 56, 42], which is typically in the following form [42], for a partially observed matrix $M \in \mathbb{R}^{m_1 \times m_2}$,

$$\min_{X,Y} \|\mathcal{P}_\Omega(M - XY^\top)\|_F^2 + \text{tr}(X^\top \mathcal{L}^{(1)}X) + \text{tr}(Y^\top \mathcal{L}^{(2)}Y) \quad (1.2)$$

where $\mathcal{L}^{(1)}$ is a graph Laplacian matrix of a graph encoding certain row-wise similarities of the data entries in M , and $\mathcal{L}^{(2)}$, likewise, is a graph Laplacian matrix for the column-wise similarities. Depending on the specific domain of application, the graph structures needed for graph regularization are either directly related to the problem background, such as traffic network of highways for road traffic prediction [30], or they can be constructed from auxiliary information, such as user communities or item similarities for online recommendation tasks [42, 18]. The usage of the graph Laplacian-based functions in (1.2) is motivated by the following reason. Given an undirected graph $\mathcal{G}^{(1)}$ on the row index set of X and a weighted graph adjacency matrix $W \in \mathbb{R}^{m_1 \times m_1}$ associated with $\mathcal{G}^{(1)}$, the Laplacian matrix of $(\mathcal{G}^{(1)}, W)$, defined as $\mathcal{L}^{(1)} = \text{diag}(W\mathbf{1}) - W$, has the following property [15, Section 1.4],

$$\text{tr}(X^\top \mathcal{L}^{(1)}X) = \sum_{i=1}^{m_1} \sum_{j=1}^{m_1} W_{ij} \|X_{i,:} - X_{j,:}\|_2^2. \quad (1.3)$$

From the form of the weighted sum of squared row-wise differences in (1.3), one can see that minimizing (1.3), subject to a constraint on X for a certain data fitting objective, promotes solutions that are piecewise smooth on the graph $\mathcal{G}^{(1)}$ [46]. More generally, the graph Laplacian-based function (1.3) is a ubiquitous tool in data analysis [16], graph signal processing [46], semi-supervised learning [2], and image restoration [40, 14, 54].

In the context of tensor completion, Narita et al. [38] considered using auxiliary graph information to regularize tensor completion solutions. They proposed tensor factorization models involving graph Laplacian regularizers for the completion of third-order tensors. The graph Laplacian regularization in [38] is designed in two ways: the first way called *cross-mode* is through a graph Laplacian-based norm of the Kronecker product of the three tensor factor matrices, and the second way called *within-mode* is through the sum of three graph Laplacian-based norms of the respective factor matrices. Other related works on tensor completion are summarized in Table 1.1, which will be further explained in Section 2.2 after the necessary notation for tensors is introduced.

TABLE 1.1

Comparison with related work on tensor completion. The column ‘ k (order)’ refers to applicability to k -th order tensors. The column ‘Cost’ refers to the dominant per-iteration cost. The column ‘Convergence’ refers to convergence result for the proposed method. ‘-’ means not available, and the check mark means the contrary. NCG refers to the nonlinear conjugate gradient method. NMF refers to nonnegative matrix factorization, and ‘*’ means additional nonnegative constraints.

	Model type	Optimization	k (order)	Cost	Graph reg.	Convergence
INDAFAC [50]	(2.7)	Gauss-Newton	3	$O((m_1 m_2 m_3)^3)$	-	-
CP-WOPT [1]	(2.7)	NCG	≥ 3	-	-	-
BPTF [52]	(2.7)	Bayesian, MCMC	3	$O(\Omega R^2)$	-	-
TNCP [34]	(2.8)	ADMM	≥ 3	$O((k+1)R\prod_{i=1}^k m_i)$	-	✓
TFAI [38]	(2.8)	EM-like, NCG	3	$O((\Omega + \text{nnz}(L))R)$	✓	✓
AirCP [22]	(2.8)	ADMM	3	-	✓	✓
FIST [31]	(2.7)*	NMF	3	$O((\Omega + \sum_{i=1}^3 m_i^2)R)$	✓	-
Ours	(2.7)	AltMin, ADMM	≥ 3	$O((\Omega + \text{nnz}(L))R)$	✓	✓

Contribution. In this paper, we address the tensor completion problem for k -th order tensors by considering a CP decomposition model (2.4) that incorporates auxiliary information via graph Laplacian regularization in the form of (1.3). The underlying CP decomposition, similar to the matrix problem (1.2) and the graph regularized problem with third-order tensors [38], has a block structure such that the search of full (m_1, \dots, m_k) -tensors can be divided into a sequence of k smaller subproblems on the CP factor spaces. Taking the graph Laplacian regularizers into account, each subproblem is formulated explicitly into a least-squares problem. Then we propose an alternating minimization algorithm (AltMin) for optimizing the graph-regularized tensor completion model. An efficient Hessian-vector multiplication scheme is adapted to a linear conjugate gradient (CG) method for solving the subproblems in the alternating minimization procedure. We provide a proof for the convergence of iterates of the proposed AltMin algorithm to a critical point of the objective function according to the Kurdyka-Łojasiewicz (KL) property.

Notice that the graph Laplacian regularization induces a coupling effect on the Hessian coefficients of each subproblem in AltMin, which complicates the resolution of the underlying least-squares problem. Therefore we consider variable splitting for the graph-regularized tensor completion model alternatively. More precisely, by splitting the CP factors in the data fitting term and the graph regularization term, we propose an alternating direction method of multipliers (ADMM), which decouples the Hessian coefficients into two splitting subproblems. One of the resulting subproblems involves a graph Laplacian term while the other does not, hence the latter one can be solved in parallel.

We conduct tensor completion experiments on both synthetic and real data and show that the proposed algorithms entail improved recovery results by using appropriate auxiliary graph information. The graph Laplacian regularization shows significant improvement on unregularized and nuclear norm-regularized models, especially when the fraction of revealed data is small. The two proposed algorithms also show speedups over several baseline methods on the synthetic and real data experiments.

Organization. We organize this paper as follows. We begin with the introduction of notations and definitions in Section 2, and we introduce the LRTC model with a graph Laplacian-based regularizer and then present several related work for CP decomposition-based tensor completion including existing methods using graph regularization. In Section 3, an alternating minimization algorithm using linear CG for solving the subproblems is proposed; an ADMM algorithm is also developed for solving the graph-regularized LRTC problem. Convergence analysis of the AltMin algorithm is given in Section 4. Numerical experiments together with some interesting observations are presented in Section 5. Conclusion is shown in Section 6.

2. Preliminaries and problem setting. In this section, we introduce the definition and notation of some tensor operations, and set up the target problem. A real-valued order- k tensor $\mathcal{Z} \in \mathbb{R}^{m_1 \times m_2 \times \dots \times m_k}$ is a multiway array in which each entry, denoted as $\mathcal{Z}_{\ell_1, \dots, \ell_k}$, is accessed via k indices $(\ell_1, \dots, \ell_k) \in [m_1] \times \dots \times [m_k]$, where $[m_i]$ denotes the index set $\{1, \dots, m_i\}$ for the integer m_i . The vector of all ones is denoted as $\mathbf{1}$ and the vector with one on the i -th entry and zeros elsewhere is denoted as \mathbf{e}_i . An $m \times m$ identity matrix is denoted as I_m .

For $k \geq 2$, the outer product of k vectors $\{u^{(1)}, \dots, u^{(k)}\}$ is a k -th order tensor, denoted as $\mathcal{Z} := u^{(1)} \circ \dots \circ u^{(k)}$, such that $\mathcal{Z}_{\ell_1, \dots, \ell_k} = u_{\ell_1}^{(1)} \dots u_{\ell_k}^{(k)}$. The *Kronecker product* of two vectors $u \in \mathbb{R}^{m_1}$ and $v \in \mathbb{R}^{m_2}$ results in a vector $u \otimes v \in \mathbb{R}^{m_1 m_2}$ defined as $u \otimes v = (u_1 v^\top, u_2 v^\top \dots u_{m_1} v^\top)^\top$. More compactly, we have $(u \otimes v)_{m_2(i-1)+j} = u_i v_j$ for $(i, j) \in [m_1] \times [m_2]$. The Kronecker product of two matrices $A \in \mathbb{R}^{m \times n}$ and $B \in \mathbb{R}^{p \times q}$ is the $pm \times qn$ matrix

$$A \otimes B = \begin{pmatrix} a_{11}B & \dots & a_{1n}B \\ \vdots & \ddots & \vdots \\ a_{m1}B & \dots & a_{mn}B \end{pmatrix}.$$

The *Khatri-Rao product* $U \odot V$ of two matrices $U \in \mathbb{R}^{m_1 \times R}$ and $V \in \mathbb{R}^{m_2 \times R}$ with the same number of columns is a matrix of size $m_1 m_2 \times R$ whose r -th column is $U_{:,r} \otimes V_{:,r}$.

For a tensor $\mathcal{Z} \in \mathbb{R}^{m_1 \times m_2 \times \dots \times m_k}$, the *mode- i matricization* $\mathcal{Z}_{(i)}$ is the $m_i \times (\prod_{j \neq i} m_j)$ unfolding matrix of \mathcal{Z} along its i -th mode. The matricization $\mathcal{Z}_{(i)}$ satisfies the following identification of the matrix entry with the tensor entry: $(\mathcal{Z}_{(i)})_{\ell_i, r_i} = \mathcal{Z}_{\ell_1, \dots, \ell_k}$ where

$$r_i = 1 + \sum_{\substack{n=1 \\ n \neq i}}^k (\ell_n - 1) I_n, \quad \text{with} \quad I_n = \prod_{\substack{j=1 \\ j \neq i}}^{n-1} m_j. \quad (2.1)$$

A *Canonical Polyadic (CP) decomposition* [24, 28, 26] of a tensor $\mathcal{Z} \in \mathbb{R}^{m_1 \times \dots \times m_k}$ is defined and denoted as

$$\mathcal{Z} = \llbracket U^{(1)}, \dots, U^{(k)} \rrbracket = \sum_{r=1}^R U_{:,r}^{(1)} \circ \dots \circ U_{:,r}^{(k)}, \quad (2.2)$$

where $U^{(i)} \in \mathbb{R}^{m_i \times R}$ for $i = 1, \dots, k$ and $R \in \mathbb{Z}$ are CP factor matrices and a rank parameter respectively satisfying (2.2). An equivalent CP form can be written as

$$\mathcal{Z}_{(i)} = U^{(i)} (U^{(k)} \circ \dots \circ U^{(i+1)} \circ U^{(i-1)} \circ \dots \circ U^{(1)})^\top = U^{(i)} ((U^{(j)})^{\circ_{j \neq i}})^\top, \quad (2.3)$$

where $\mathcal{Z}_{(i)}$ is the mode- i tensor matricization. Given an index $i \in [k]$, the subscript or superscript $(-i)$ means that the notion in question depends on the subset (or filtering) $[k] \setminus \{i\}$. Hence the following notations, $m_{(-i)} := \prod_{j \neq i} m_j$ and $U^{(-i)} := (U^{(j)})^{\circ_{j \neq i}} \in \mathbb{R}^{m_{(-i)} \times R}$, are used for brevity whenever needed.

The Frobenius inner product of two matrices A, B of the same size, by definition, is denoted by $\langle A, B \rangle = \text{tr}(A^\top B)$ interchangeably. The *tensor inner product* of two tensors $\mathcal{Z}^{(1)}, \mathcal{Z}^{(2)} \in \mathbb{R}^{m_1 \times m_2 \times \dots \times m_k}$ of the same size is defined as

$$\langle \mathcal{Z}^{(1)}, \mathcal{Z}^{(2)} \rangle = \sum_{\ell_1=1}^{m_1} \dots \sum_{\ell_k=1}^{m_k} \mathcal{Z}_{\ell_1 \dots \ell_k}^{(1)} \mathcal{Z}_{\ell_1 \dots \ell_k}^{(2)}.$$

The Frobenius norm of a tensor $\mathcal{Z} \in \mathbb{R}^{m_1 \times m_2 \times \dots \times m_k}$, same as the matrix notation, is defined and denoted as $\|\mathcal{Z}\|_F = \sqrt{\langle \mathcal{Z}, \mathcal{Z} \rangle}$.

2.1. Problem setting. We introduce our LRTC model in the form of CP decomposition with a graph Laplacian-based regularization,

$$\min_{U^{(1)}, \dots, U^{(k)}} \frac{1}{2} \|\mathcal{P}_\Omega(\mathcal{T} - \llbracket U^{(1)}, \dots, U^{(k)} \rrbracket)\|_F^2 + \sum_{i=1}^k \frac{\lambda_i}{2} \text{tr}((U^{(i)})^\top L^{(i)} U^{(i)}) + \sum_{i=1}^k \frac{\lambda_i}{2} \|(U^{(j)})^{\circ_{j \neq i}}\|_F^2 \quad (2.4)$$

where $U := (U^{(1)}, \dots, U^{(k)}) \in \mathbb{R}^{m_1 \times R} \times \dots \times \mathbb{R}^{m_k \times R}$ for a (strictly positive) rank parameter R , Ω denotes the index set of the revealed tensor entries ($\Omega \subset [m_1] \times \dots \times [m_k]$) and \mathcal{T} is the tensor that is revealed only on Ω . The proportion of the revealed entries $\frac{|\Omega|}{m_1 \dots m_k}$ is referred to as the *sampling rate*. The shifted graph Laplacian $L^{(i)}$ is defined as

$$L^{(i)} = \lambda_L \mathcal{L}^{(i)} + I_{m_i} \quad \text{with} \quad \mathcal{L}^{(i)} = \text{diag}(W^{(i)} \mathbf{1}) - W^{(i)}, \quad (2.5)$$

where $W^{(i)}$ is a weighted adjacency matrix of a given graph $\mathcal{G}^{(i)}$ on the index set $[m_i]$, i.e., $W_{\ell_1, \ell_2}^{(i)} \neq 0$ if and only if (ℓ_1, ℓ_2) is an (undirected) edge of $\mathcal{G}^{(i)}$. The Frobenius norm-based terms in the regularizer of (2.4) (when $\lambda_i > 0$ and $\lambda_L = 0$) are related to the nuclear norm of the matricizations of \mathcal{Z} through the following characterization [47]:

$$\|\mathcal{Z}_{(i)}\|_* = \min_{U^{(i)} ((U^{(j)})^{\circ_{j \neq i}})^\top = \mathcal{Z}_{(i)}} \frac{1}{2} \{\|U^{(i)}\|_F^2 + \|(U^{(j)})^{\circ_{j \neq i}}\|_F^2\}. \quad (2.6)$$

In the general case ($\lambda_i > 0$ and $\lambda_L > 0$), the regularizer of (2.4) can be seen as a generalized form of the nuclear norm (2.6), which entails a generalization of the tensor nuclear norm.

The parameters λ_i and λ_L control the trade-off between the regularization term and the data fitting term. More specifically, the graph Laplacian-based regularization term, as explained in (1.3), has the effect of favoring solutions that tend to be piecewise smooth with respect to the graph links in $\mathcal{G}^{(i)}$. Therefore, the regularization of (2.4) (for $\lambda_L > 0$) induces a trade-off between data fitting on the revealed entries and piecewise smoothness according to the given graph across the whole index set. In particular, when $\lambda_L = 0$, problem (2.4) reduces to a Frobenius norm-regularized tensor completion model (for $\lambda_i > 0$) or an unregularized model (for $\lambda_i = 0$).

2.2. Related work. Among the prior work on LRTC using CP decomposition, we give a representative list of methods, including ours, that deal with either of the following two tensor completion models (while some methods are limited to third-order tensors):

$$\min_U \|P_\Omega(\llbracket U^{(1)}, \dots, U^{(k)} \rrbracket) - \mathcal{T}\|_F^2 + \psi(U); \quad (2.7)$$

$$\min_{\hat{\mathcal{T}}, U} \|\hat{\mathcal{T}} - \llbracket U^{(1)}, \dots, U^{(k)} \rrbracket\|_F^2 + \psi(U) \quad \text{subject to} \quad \mathcal{P}_\Omega(\hat{\mathcal{T}}) = \mathcal{P}_\Omega(\mathcal{T}), \quad (2.8)$$

where ψ is a (possibly zero-valued) regularizer.

A comparison with existing methods is given in Table 1.1. Our work considers (2.4) with general k -th order tensors, which is of type (2.7) where the graph Laplacian-based regularizer (1.3) is enabled. The proposed algorithms (AltMin and ADMM) have per-iteration costs less than or comparable to others, and the convergence property of AltMin is given. INDAFAC is a damped Gauss-Newton method proposed by Tomasi and Bro [50] for solving (2.7) with $\psi = 0$. CP-WOPT is an algorithm by Acar et al. [1] for solving (2.7) with $\psi = 0$, and is available in the Tensor Toolbox [4]. BPTF is a Bayesian probabilistic tensor CPD algorithm by Xiong et al. [52] for solving (2.7) where the regularizer ψ is composed of Frobenius norms of the factors of U and an ℓ_2 norm-based function imposing columnwise smoothness of $U^{(3)}$. TFAI is an algorithm for optimizing the auxiliary-information model of Narita et al. [38], which corresponds to (2.8) where ψ is a graph Laplacian-based regularizer (in the within-mode) as in (2.4). TNCP is an ADMM algorithm by Liu et al. [34] for solving a matrix trace-norm regularized problem, which is transformed into the form of (2.8) where $\psi(U) = \sum_{i=1}^3 \alpha_i \|U^{(i)}\|_*$. AirCP is an ADMM algorithm by Ge et al. [22] for solving (2.8) where ψ takes the form of $\psi(U, X)$ —under equality constraints $U^{(i)} = X^{(i)}$ —and is composed of the sum of Frobenius norms of $U^{(i)}$ and the graph Laplacian-based norms of $X^{(i)}$. FIST is a nonnegative matrix factorization (NMF) method by Li et al. [31] for solving (2.7) with additional nonnegative constraints on all three CP factors $U^{(i)}$, where ψ is the graph Laplacian-based function (1.3) of the vectorization of the (third-order) candidate tensor.

3. Algorithms. In this section, we introduce an alternating minimization (AltMin) algorithm and an ADMM algorithm for solving the LRTC problem (2.4).

3.1. Alternating minimization. To minimize the objective function of (2.4), defined on the product space of CP factors $\mathbb{R}^{m_1 \times R} \times \dots \times \mathbb{R}^{m_k \times R}$, alternating minimization (also referred to as block coordinate descent) consists in minimizing the function cyclically over each factor matrix among $(U^{(1)}, \dots, U^{(k)})$ while keeping the remaining variables fixed at their last updated values.

Let $f(\cdot)$ denote the objective function of (2.4). We consider the optimization problem on the product space, i.e., $\min_{U^{(1)}, \dots, U^{(k)}} f(U^{(1)}, \dots, U^{(k)})$. Given the t -th iterate $(U_t^{(1)}, \dots, U_t^{(k)})$, the (cyclic) alternating minimization resorts to solving the following sequence of subproblems for $i = 1, \dots, k$,

$$\min_{U^{(i)} \in \mathbb{R}^{m_i \times R}} f_{t+1}^{(i)}(U^{(i)}) := f(U_{t+1}^{(1)}, \dots, U_{t+1}^{(i-1)}, U^{(i)}, U_t^{(i+1)}, \dots, U_t^{(k)}), \quad (3.1)$$

where $f_{t+1}^{(i)}$ denotes the objective function of the subproblem in $U^{(i)}$. The procedure of alternating minimization is listed in Algorithm 1.

Algorithm 1 Alternating minimization (AltMin) for solving (2.4)

Input: Data (revealed on Ω) $\mathcal{P}_\Omega(\mathcal{T}) \in \mathbb{R}^{m_1 \times \dots \times m_k}$, observed set Ω . Objective function f

Output: $(U_t^{(i)})_{i=1, \dots, k}$

- 1: Initialization: $U_0^{(1)}, \dots, U_0^{(k)}$
 - 2: **for** $t = 0, 1, 2, \dots$ **do**
 - 3: **if** stopping criterion is satisfied **then**
 - 4: **return**;
 - 5: **end if**
 - 6: **for** $i = 1, \dots, k$ **do**
 - 7: $U_{t+1}^{(i)} = \arg \min_{U^{(i)} \in \mathbb{R}^{m_i \times R}} f_{t+1}^{(i)}(U^{(i)})$
 - 8: **end for**
 - 9: **end for**
-

Alternating subproblems. Due to the graph Laplacian-based regularization term, the major challenge in solving (2.4) by the alternating minimization procedure is the structure of each subproblem (3.1), which is different from those of an unregularized tensor decomposition problem. Specifically, during the $(t + 1)$ -th iteration and for $i \in [k]$, the minimization (3.1) has the following explicit expression¹:

$$\min_{U^{(i)} \in \mathbb{R}^{m_i \times R}} \frac{1}{2} \|\mathcal{P}_{\Omega^{(i)}}(\mathcal{T}_{(i)} - U^{(i)}((U^{(j)})^{\odot_{j \neq i}})^{\top})\|_{\mathbb{F}}^2 + \frac{\lambda_i}{2} \text{tr}((U^{(i)})^{\top} L^{(i)} U^{(i)}) + \sum_{\substack{j=1 \\ j \neq i}}^k \frac{\lambda_j}{2} \|(U^{(n)})^{\odot_{n \neq j}}\|_{\mathbb{F}}^2 \quad (3.2)$$

where the first term is transformed from the mode- i matricization (2.3), and $\Omega^{(i)}$ is the set of 2-dimensional indices of the form (ℓ_i, r_i) , which is transformed from the tensor index $(\ell_1, \dots, \ell_k) \in \Omega$ via (2.1) after the mode- i matricization (Section 2). In fact, the subproblem (3.1) has a quadratic objective.

PROPOSITION 3.1. *Let $\mathbf{x} := \text{vec}((U^{(i)})^{\top}) \in \mathbb{R}^{m_i R}$ be the vectorization of $(U^{(i)})^{\top}$, and let $g^{(i)}(\mathbf{x}) := f_{t+1}^{(i)}(U^{(i)})$ defined in (3.1). Then $g^{(i)}$ is a quadratic function of the following form,*

$$g^{(i)}(\mathbf{x}) := \frac{1}{2} \mathbf{x}^{\top} M^{(i)} \mathbf{x} - \text{vec}(Q^{(i)})^{\top} \mathbf{x} \quad \text{with} \quad (3.3)$$

$$M^{(i)} := A^{(i)} + I_{m_i} \otimes C^{(i)} + \lambda_i L^{(i)} \otimes I_R \quad (3.4)$$

$$Q^{(i)} := (\mathcal{P}_{\Omega^{(i)}}(\mathcal{T}_{(i)}))(U^{(j)})^{\odot_{j \neq i}}, \quad (3.5)$$

where $A^{(i)} = \sum_{s=1}^{m_i} (\mathbf{e}_s \mathbf{e}_s^{\top}) \otimes A_s^{(i)} \in \mathbb{R}^{m_i R \times m_i R}$ is such that the $R \times R$ blocks are

$$A_s^{(i)} = \sum_{\ell \in \Omega_s^{(i)}} (U_{\ell, :}^{(-i)})^{\top} U_{\ell, :}^{(-i)} \quad \text{for } s \in [m_i] \text{ and } \Omega_s^{(i)} = \{\ell : (s, \ell) \in \Omega^{(i)}\}, \quad (3.6)$$

and $C^{(i)} \in \mathbb{R}^{R \times R}$ writes

$$C^{(i)} = \sum_{\substack{j=1 \\ j \neq i}}^k \lambda_j \text{diag}(\|U_{:, \ell}^{(-i, -j)}\|^2)_{\ell=1, \dots, R} \quad \text{for } U^{(-i, -j)} := (U^{(n)})^{\odot_{n \neq i, j}}, \quad (3.7)$$

where $(U^{(n)})^{\odot_{n \neq i, j}}$ denotes the Khatri-Rao product of $U^{(n)}$'s excluding $U^{(i)}$ and $U^{(j)}$.

¹For convenience, we ignore the subscript $t + 1$ or t in the variables $U^{(j)}$ for all $j = 1, \dots, k$, and omit constant terms in the objective.

Proof. Given the vectorization $\mathbf{x} = \text{vec}((U^{(i)})^\top)$, the term $L^{(i)} \otimes I_R$ in (3.4) is obtained due to the relation $(B^\top \otimes A)\text{vec}(X) = \text{vec}(AXB)$. The components $A^{(i)}$ and $C^{(i)}$ in (3.4) are defined and computed as follows. Let $A^{(i)} \in \mathbb{R}^{m_i R \times m_i R}$ be the matrix of the quadratic form $\mathbf{x}^\top A^{(i)} \mathbf{x} := \|\mathcal{P}_{\Omega^{(i)}}(U^{(i)}((U^{(j)})^{\odot_{j \neq i}})^\top)\|_F^2$ in \mathbf{x} . Notice that

$$\begin{aligned} \mathbf{x}^\top A^{(i)} \mathbf{x} &:= \|\mathcal{P}_{\Omega^{(i)}}(U^{(i)}((U^{(j)})^{\odot_{j \neq i}})^\top)\|_F^2 = \langle U^{(i)}(U^{(-i)})^\top, P_{\Omega^{(i)}}(U^{(i)}(U^{(-i)})^\top) \rangle \\ &= \text{tr} \left(U^{(-i)} U^{(i)^\top} P_{\Omega^{(i)}}(U^{(i)}(U^{(-i)})^\top) \right) = \sum_{s=1}^{m_i} U^{(-i)} U_{s,:}^\top P_{\Omega_s^{(i)}}(U_{s,:}(U^{(-i)})^\top) \\ &= \sum_{s=1}^{m_i} U_{s,:}(U^{(-i)})^\top P_{\Omega_s^{(i)}}(U^{(-i)}) U_{s,:}^\top = \sum_{s=1}^{m_i} U_{s,:} \left(\sum_{\ell \in \Omega_s^{(i)}} (U_{\ell,:}^{(-i)})^\top U_{\ell,:}^{(-i)} \right) U_{s,:}^\top \end{aligned} \quad (3.8)$$

where $U_{s,:}$ denotes the s -th row of $U^{(i)}$ and $U^{(-i)} := (U^{(j)})^{\odot_{j \neq i}}$ is used for clarity (see Section 2). Equation (3.8) holds because the projection $P_{\Omega_s^{(i)}}$ (defined on $\mathbb{R}^{m^{(-i)}}$ by default) applies to each of the columns of $U^{(-i)}$, which has the effect of projecting any row of $U^{(-i)}$ with index $\ell \notin \Omega_s^{(i)}$ to a row of zeros. Therefore, $A^{(i)} \in \mathbb{R}^{m_i R \times m_i R}$ is a block diagonal matrix with m_i diagonal blocks and each block has the form

$$A_s^{(i)} = \sum_{\ell \in \Omega_s^{(i)}} (U_{\ell,:}^{(-i)})^\top U_{\ell,:}^{(-i)} \quad \text{for } s \in [m_i],$$

where $\Omega_s^{(i)} = \{\ell : (s, \ell) \in \Omega^{(i)}\}$.

Now we verify (3.7). The component $I_{m_i} \otimes C^{(i)}$ denotes the matrix related to the third term in (3.2): $q(U^{(i)}) := \sum_{j \in [k], j \neq i} \lambda_j \|(U^{(n)})^{\odot_{n \neq j}}\|_F^2$, which satisfies

$$\begin{aligned} q(U^{(i)}) &= \sum_{j \neq i} \lambda_j \sum_{\ell=1}^R \|U_{\ell,:}^{(-i,-j)} \otimes U_{\ell,:}^{(i)}\|_2^2 = \sum_{j \neq i} \lambda_j \sum_{\ell=1}^R \underbrace{\|U_{\ell,:}^{(-i,-j)}\|_2^2}_{C_{\ell\ell}^{(i,j)}} \text{tr}(U_{\ell,:}^{(i)}(U_{\ell,:}^{(i)})^\top) \\ &= \sum_{j \neq i} \lambda_j \text{tr}(U^{(i)} C^{(i,j)} (U^{(i)})^\top) = \text{tr}(U^{(i)} (\sum_{j \neq i} \lambda_j C^{(i,j)}) (U^{(i)})^\top). \end{aligned}$$

Finally, since $\text{tr}(X^\top CX) = \text{vec}(X)^\top (I \otimes C) \text{vec}(X)$, the expression of $C^{(i)}$ (3.7) yields the identification $q(U^{(i)}) = \mathbf{x}^\top (I_{m_i} \otimes C^{(i)}) \mathbf{x}$ for $\mathbf{x} = \text{vec}((U^{(i)})^\top)$. \square

The function $g^{(i)}$ in (3.3), and equivalently $f_{t+1}^{(i)}$ of (3.2), is strongly convex (see the proof of Theorem 4.7) provided that $\lambda_i > 0$ for $i = 1, \dots, k$. In fact, solving the minimization (3.2) can be rewritten as the following quadratic minimization problem

$$\min_{\mathbf{x} \in \mathbb{R}^{m_i R}} g^{(i)}(\mathbf{x}) = \frac{1}{2} \mathbf{x}^\top M^{(i)} \mathbf{x} - \text{vec}(Q^{(i)})^\top \mathbf{x}. \quad (3.9)$$

We consider linear CG for solving problem (3.9). Algorithm 2 called AltMin-CG is an adaptation of AltMin (Algorithm 1) using linear CG as the subproblem solver. In Algorithm 2 (line 9), $\text{unvec}(\cdot)$ is the operation of turning the $m_i R$ -dimensional vector into an $R \times m_i$ matrix (in the column-major way).

The linear CG solver. Detailed steps for the linear CG adaptation are given in Algorithm 3. Note that the matrix-vector product $M^{(i)} \mathbf{x}$ appearing in the linear CG subroutine (Algorithm 3, line 12) dominates the computational cost since $M^{(i)}$ is a matrix of size $m_i R \times m_i R$. To overcome this computational bottleneck, we take advantage of the structure of $M^{(i)} = A^{(i)} + I_{m_i} \otimes C^{(i)} + \lambda_i L^{(i)} \otimes I_R$ in (3.4) and propose a more efficient way by the following special Hessian-vector multiplication. Recall that $(B^\top \otimes A)\text{vec}(X) = \text{vec}(AXB)$, it

Algorithm 2 AltMin-CG for solving (2.4)

Input: Observed tensor $\mathcal{P}_\Omega(\mathcal{T})$, graph Laplacian $\mathcal{L}^{(1)}, \dots, \mathcal{L}^{(k)}$, observed set Ω , parameters $\lambda_1, \dots, \lambda_k > 0$ and $\lambda_L \geq 0$

Output: $(U_t^{(i)})_{i=1, \dots, k}$

- 1: Initialization: $U_0^{(1)}, \dots, U_0^{(k)}$
- 2: **for** $t = 0, 1, 2, \dots$ **do**
- 3: **if** stopping criterion is satisfied **then**
- 4: return;
- 5: **end if**
- 6: **for** $i = 1, \dots, k$ **do**
- 7: Compute: $C^{(i)}, Q^{(i)}$ defined in (3.7), (3.5) and $(U^{(j)})^{\odot_{j \neq i}}$
- 8: Get $\mathbf{x}_{t+1}^{(i)}$ by approximately solving $\min_{\mathbf{x}} g^{(i)}(\mathbf{x})$ (3.9) # see Algorithm 3
- 9: $U_{t+1}^{(i)} = (\text{unvec}(\mathbf{x}_{t+1}^{(i)}))^{\top}$
- 10: **end for**
- 11: **end for**

Algorithm 3 Linear CG for solving (3.9)

Input: $M^{(i)} \in \mathbb{R}^{m_i R \times m_i R}$, $Q^{(i)} \in \mathbb{R}^{m_i \times R}$, initial point $\mathbf{x}_0 \in \mathbb{R}^{m_i R}$, accuracy parameter ϵ , iteration budget T_{\max}

Output: $\mathbf{x}_t \in \mathbb{R}^{m_i R}$

- 1: $\mathbf{r}_0 = \text{vec}(Q^{(i)}) - M^{(i)} \mathbf{x}_0$
- 2: **for** $t = 0, \dots, T_{\max}$ **do**
- 3: Compute: $\|\mathbf{r}_t\|$
- 4: **if** $\|\mathbf{r}_t\| \leq \epsilon \|\mathbf{r}_0\|$ **then**
- 5: Break
- 6: **end if**
- 7: **if** $t = 0$ **then**
- 8: $\mathbf{p}_1 = \mathbf{r}_0$
- 9: **else**
- 10: $\mathbf{p}_{t+1} = \mathbf{r}_t + \frac{\|\mathbf{r}_t\|^2}{\|\mathbf{r}_{t-1}\|^2} \mathbf{p}_t$
- 11: **end if**
- 12: Compute: $\mathbf{v}_{t+1} = M^{(i)} \mathbf{p}_{t+1}$ # see Algorithm 4
- 13: Compute: $\alpha = \frac{\|\mathbf{r}_t\|^2}{\mathbf{p}_{t+1}^{\top} \mathbf{v}_{t+1}}$
- 14: Compute: $\mathbf{x}_{t+1} = \mathbf{x}_t + \alpha \mathbf{p}_{t+1}$, $\mathbf{r}_{t+1} = \mathbf{r}_t - \alpha \mathbf{v}_{t+1}$
- 15: **end for**

follows from $\mathbf{x} = \text{vec}((U^{(i)})^{\top})$ that

$$\begin{aligned} (L^{(i)} \otimes I_R) \mathbf{x} &= \text{vec}((U^{(i)})^{\top} L^{(i)}), \\ (I_{m_i} \otimes C^{(i)}) \mathbf{x} &= \text{vec}(C^{(i)} (U^{(i)})^{\top}). \end{aligned}$$

Thus the larger Hessian-vector multiplication can be implemented by a series of smaller matrix multiplications as follows

$$M^{(i)} \mathbf{x} = \text{vec}(\lambda_i (U^{(i)})^{\top} L^{(i)} + C^{(i)} (U^{(i)})^{\top}) + A^{(i)} \mathbf{x}. \quad (3.10)$$

For the computation of $A^{(i)} \mathbf{x}$ in (3.10), we make use of the block diagonal structure of $A^{(i)}$ specified

Algorithm 4 Hessian-vector multiplication $M^{(i)}\mathbf{x}$ in the CG method

Input: $L^{(i)} \in \mathbb{R}^{m_i \times m_i}$, $\Omega_j^{(i)} \in \mathbb{R}^{R \times R}$, $C^{(i)} \in \mathbb{R}^{R \times R}$, $U^{(-i)} := (U^{(j)})^{\odot_{j \neq i}} \in \mathbb{R}^{m_{(-i)} \times R}$, $\mathbf{x} := \text{vec}((U^{(i)})^\top) \in \mathbb{R}^{m_i R}$, $\lambda_i \geq 0$.

Output: $M^{(i)}\mathbf{x}$

- 1: $X = \text{unvec}(\mathbf{x}) \in \mathbb{R}^{R \times m_i}$
 - 2: **for** $j = 1, \dots, m_i$ **do**
 - 3: Compute $N_{:,j}^{(i)} = \sum_{\ell \in \Omega_j^{(i)}} (U_{\ell,:}^{(-i)} X_{:,j}) (U_{\ell,:}^{(-i)})^\top$
 - 4: **end for**
 - 5: Compute: $M^{(i)}\mathbf{x} = \text{vec}(C^{(i)}X + \lambda_i X L^{(i)}) + \text{vec}(N^{(i)})$ defined in (3.10)
-

in (3.6). More precisely, let

$$N_{:,j}^{(i)} := A_j^{(i)} (U_{j,:}^{(i)})^\top = \sum_{\ell \in \Omega_j^{(i)}} (U_{\ell,:}^{(-i)} (U_{j,:}^{(i)})^\top) (U_{\ell,:}^{(-i)})^\top \quad \text{for } j \in [m_i].$$

Then we have

$$A^{(i)}\mathbf{x} = A^{(i)}\text{vec}((U^{(i)})^\top) = \text{vec}(N^{(i)}) = \text{vec}((N_{:,1}^{(i)}, \dots, N_{:,m_i}^{(i)})), \quad (3.11)$$

where the computation of each $N_{:,j}^{(i)}$ can be done in parallel. Details to compute the Hessian-vector product in the CG method are listed in Algorithm 4.

Computational cost of AltMin-CG. The computational cost for each alternating step (3.2) corresponds to the procedure required by line 7–line 9 of Algorithm 2.

The cost of forming $(U^{(j)})^{\odot_{j \neq i}}$ is $O(\frac{|\Omega|R}{\rho m_i})$, where ρ denotes the sampling rate. The cost of computing $Q^{(i)}$ in (3.5) is $O(|\Omega|R)$ with access to $(U^{(j)})^{\odot_{j \neq i}}$. The cost of forming $C^{(i)}$ in (3.7) is $O(\frac{|\Omega|R}{\rho m_i m_j})$.

The major cost in Algorithm 2 corresponds to line 8, which involves (inner) iterations of the linear CG. The total cost of line 8 is n_{CG} times the per-iteration cost of the linear CG algorithm (Algorithm 3), where n_{CG} denotes the number of iterations required by the CG solver (Algorithm 3) for producing $\mathbf{x}_{t+1}^{(i)}$. The per-iteration cost of Algorithm 3 is mainly composed of the following components.

- Cost of computing $A^{(i)}\mathbf{x}$: $O(|\Omega|R)$, since the cost of computing $A_j^{(i)}(u_{j,:}^{(i)})^\top$ in (3.11) is $O(|\Omega_j^{(i)}|R)$ for $j = 1, \dots, m_i$ and $\sum_{j=1, \dots, m_i} |\Omega_j^{(i)}| = |\Omega|$;
- Cost of computing $(L^{(i)} \otimes I_R)\mathbf{x}$: $O(\text{nnz}(L^{(i)})R)$;
- Cost of computing $(I_{m_i} \otimes C^{(i)})\mathbf{x}$: $O(m_i R)$.

Hence, the cost of computing the Hessian-vector multiplication $M^{(i)}\mathbf{x}$ is $O(\text{nnz}(L^{(i)})R + |\Omega|R)$. The number of linear CG iterations needed is theoretically bounded by the problem dimension; and in practice, we limit this number by a constant iteration budget. Therefore the dominant per-iteration cost of Algorithm 2 is

$$O((\text{nnz}(L^{(i)}) + |\Omega|)R).$$

REMARK 3.2. *The main computational challenge in finding the solution of (3.9) is the presence of graph Laplacian-based regularization terms in $M^{(i)} \in \mathbb{R}^{m_i R \times m_i R}$. The similar difficulty can be found in the graph-regularized least squares problem in [42]. More precisely, the matrix $M^{(i)} = A^{(i)} + I_{m_i} \otimes C^{(i)} + \lambda_i L^{(i)} \otimes I_R$ is not block diagonal, due to the fact that the component $L^{(i)} \otimes I_R$ is not block diagonal, since $L^{(i)}$ defined in (2.5) has nonzeros—corresponding to the edges of the graph $\mathcal{G}^{(i)}$ —on its off-diagonal terms. Therefore, the minimization problem (3.9) cannot be decomposed into m_i separable smaller problems in \mathbb{R}^R .*

In light of Remark 3.2, we also consider an alternating direction method of multipliers (ADMM) as an alternative way to address the difficulty with this nonseparable quadratic problem.

3.2. ADMM. Besides AltMin-CG, we adapt an ADMM algorithm [22] to solve the graph-regularized problem (2.4) whose objective consists of three terms: the data fitting term, the graph regularizers, and the Frobenius norm-based regularizers. The advantage of ADMM lies in that it decomposes complex optimization problems into sequences of simpler subproblems and that it splits coupling constraints by a dual multiplier. (Another reason for its popularity is that, if the objective function is strongly convex—which is not the case of (2.4)—and Lipschitz continuous, then with appropriate choice of parameters ADMM will convergence linearly.) For nonconvex problems, ADMM can be considered as a local minimization method, and the hope is that it will possibly have better convergence properties than other local optimization methods [9].

Since $L^{(i)}$ brings about the coupling effect to the quadratic minimization problem underlying (2.4), we introduce $B^{(i)}$ as an auxiliary variable that equals $U^{(i)}$ to decouple the regularization terms in problem (2.4) as follows

$$\begin{aligned} \min_{U^{(1)}, \dots, U^{(k)}} \quad & \frac{1}{2} \|\mathcal{P}_\Omega(\mathcal{T} - \llbracket U^{(1)}, \dots, U^{(k)} \rrbracket)\|_{\mathbb{F}}^2 + \sum_{i=1}^k \frac{\lambda_i}{2} \text{tr}((B^{(i)})^\top L^{(i)} B^{(i)}) + \sum_{i=1}^k \frac{\lambda_i}{2} \|(U^{(j)})^{\odot_{j \neq i}}\|_{\mathbb{F}}^2, \\ \text{subject to} \quad & U^{(i)} = B^{(i)}, \text{ for } i = 1, \dots, k. \end{aligned} \quad (3.12)$$

Then the augmented Lagrangian for the above optimization problem (3.12) is

$$\mathcal{L}_\eta(U, B, Y) = f(U, B) + \sum_{i=1}^k \langle Y^{(i)}, B^{(i)} - U^{(i)} \rangle + \sum_{i=1}^k \frac{\eta}{2} \|B^{(i)} - U^{(i)}\|_{\mathbb{F}}^2, \quad (3.13)$$

where $f(U, B)$ denotes the objective function of (3.12), $Y^{(i)} \in \mathbb{R}^{m_i \times R}$ are the Lagrange multipliers, and $\eta > 0$ is a penalty parameter. Given the current iterates U_t and B_t , applying the ADMM iterative scheme successively to minimize \mathcal{L}_η over $\{U^{(1)}, \dots, U^{(k)}\}$ and $\{B^{(1)}, \dots, B^{(k)}\}$ turns out to

$$\{U_{t+1}^{(1)}, \dots, U_{t+1}^{(k)}\} = \arg \min_{U^{(1)}, \dots, U^{(k)}} \mathcal{L}_{\eta_t}(U^{(1)}, \dots, U^{(k)}, B_t^{(1)}, \dots, B_t^{(k)}, Y_t^{(1)}, \dots, Y_t^{(k)}), \quad (3.14)$$

$$\{B_{t+1}^{(1)}, \dots, B_{t+1}^{(k)}\} = \arg \min_{B^{(1)}, \dots, B^{(k)}} \mathcal{L}_{\eta_t}(U_{t+1}^{(1)}, \dots, U_{t+1}^{(k)}, B^{(1)}, \dots, B^{(k)}, Y_t^{(1)}, \dots, Y_t^{(k)}), \quad (3.15)$$

$$Y_{t+1}^{(i)} = Y_t^{(i)} + \eta_t(B_{t+1}^{(i)} - U_{t+1}^{(i)}), \quad i = 1, \dots, k. \quad (3.16)$$

Next we consider solving these subproblems step by step.

Updating $\{U_{t+1}^{(1)}, \dots, U_{t+1}^{(k)}\}$: The optimization problem (3.14) can be rewritten as follows when updating $\{U_{t+1}^{(1)}, \dots, U_{t+1}^{(k)}\}$

$$\min_{U^{(1)}, \dots, U^{(k)}} \frac{1}{2} \|\mathcal{P}_\Omega(\mathcal{T} - \llbracket U^{(1)}, \dots, U^{(k)} \rrbracket)\|_{\mathbb{F}}^2 + \sum_{i=1}^k \frac{\lambda_i}{2} \|(U^{(j)})^{\odot_{j \neq i}}\|_{\mathbb{F}}^2 + \sum_{i=1}^k \frac{\eta_t}{2} \|U^{(i)} - B_t^{(i)} - (1/\eta_t)Y_t^{(i)}\|_{\mathbb{F}}^2. \quad (3.17)$$

We apply the alternating minimization method to update each $U^{(i)}$ for $i = 1, \dots, k$, while fixing the other variables. Then problem (3.17) becomes a quadratic optimization problem. For convenience, we ignore the subscript in the fixed $U^{(j)}$ for $j \neq i$, and the resulting subproblem with respect to $U^{(i)}$ is formulated as

$$\min_{U^{(i)}} \frac{1}{2} \|\mathcal{P}_{\Omega^{(i)}}(\mathcal{T}_{(i)} - U^{(i)}((U^{(j)})^{\odot_{j \neq i}})^\top)\|_{\mathbb{F}}^2 + \sum_{\substack{j=1 \\ j \neq i}}^k \frac{\lambda_j}{2} \|(U^{(n)})^{\odot_{n \neq j}}\|_{\mathbb{F}}^2 + \frac{\eta_t}{2} \|U^{(i)} - B_t^{(i)} - \frac{Y_t^{(i)}}{\eta_t}\|_{\mathbb{F}}^2, \quad (3.18)$$

which is separable by rows of $U^{(i)}$. Thus, each row of the new iterate $U_{t+1}^{(i)}$ is the solution to the following linear equation in \mathbb{R}^R ,

$$(A_j^{(i)} + \eta_t I_R + C^{(i)})(U_{j,:}^{(i)})^\top = ((\mathcal{P}_{\Omega^{(i)}}(\mathcal{T}_{(i)}))(U^{(j)})^{\odot_{j \neq i}} + \eta_t B_t^{(i)} + Y_t^{(i)})_{j,:}^\top, \quad (3.19)$$

where $A_j^{(i)}$ and $C^{(i)}$ are defined in (3.6) and (3.7) respectively, for $j = 1, \dots, m_i$.

Updating $\{B_{t+1}^{(1)}, \dots, B_{t+1}^{(k)}\}$: By alternating minimization method, the optimization problem (3.15) can be reformulated as follows when updating the variables $\{B_{t+1}^{(1)}, \dots, B_{t+1}^{(k)}\}$,

$$\min_{B^{(i)}} \lambda_i \operatorname{tr}((B^{(i)})^\top L^{(i)} B^{(i)}) + \eta_t \|U_{t+1}^{(i)} - B^{(i)} - (1/\eta_t) Y_t^{(i)}\|_{\mathbb{F}}^2, \quad (3.20)$$

which boils down to solving the linear equation,

$$(\eta_t I_{m_i} + \lambda_i L^{(i)}) B^{(i)} = \eta_t U_{t+1}^{(i)} - Y_t^{(i)}. \quad (3.21)$$

To update $B_{t+1}^{(i)}$ in (3.21), we adopt the CG method (Algorithm 3) combined with the Hessian-vector product presented in Section 3.1. Similarly, the iterate $U_{t+1}^{(i)}$ in (3.19) is updated by rows using the same CG method.

In summary, the above procedures are presented in Algorithm 5.

Algorithm 5 ADMM for solving (2.4)

Input: Observed tensor $\mathcal{P}_\Omega(\mathcal{T})$, graph Laplacian $\mathcal{L}^{(1)}, \dots, \mathcal{L}^{(k)}$, observed set Ω , parameters γ , η_{\max} , $\lambda_1, \dots, \lambda_k$ and λ_L

Output: $(U_t^{(i)})_{i=1, \dots, k}$

- 1: Initialization: $U_0^{(1)}, \dots, U_0^{(k)}, \eta_0$
 - 2: **for** $t = 0, 1, 2, \dots$, **do**
 - 3: **if** stopping criterion is satisfied **then**
 - 4: Break
 - 5: **end if**
 - 6: **for** $i = 1, \dots, k$ **do**
 - 7: **for** $j = 1, \dots, m_i$ **do**
 - 8: Update the j -th row of $U_{t+1}^{(i)}$ by solving (3.19)
 - 9: **end for**
 - 10: Update $B_{t+1}^{(i)}$ by solving (3.21)
 - 11: $Y_{t+1}^{(i)} = Y_t^{(i)} + \eta_t^{(i)} (B_{t+1}^{(i)} - U_{t+1}^{(i)})$
 - 12: **end for**
 - 13: Update $\eta_{t+1} = \min(\gamma \eta_t, \eta_{\max})$
 - 14: **end for**
-

Computational cost of ADMM. We analyze the computational cost for each alternating step of the augmented Lagrangian step (3.13) corresponding to the procedure required by line 6–line 12 of Algorithm 5. The costs of forming $(U^{(j)})^{\odot_{j \neq i}}$, $C^{(i)}$ and $Q^{(i)}$ are computed in the complexity analysis part of Section 3.1. The dominant costs for solving the linear equations (3.19) and (3.21) are $\tilde{n}_{\text{CG}}(m_i + |\Omega|)R$ and $\tilde{n}_{\text{CG}} \operatorname{nnz}(L^{(i)})R$ respectively, where \tilde{n}_{CG} denotes the maximal number of iterations required for solving the linear equations (3.19) and (3.21). Similar to AltMin-CG, the number \tilde{n}_{CG} is theoretically bounded by the problem dimension, and in practice, is limited by a constant iteration budget, the per-iteration cost of Algorithm 5 (ADMM) is

$$O((\operatorname{nnz}(L^{(i)}) + |\Omega|)R),$$

which is of the same order as Algorithm 2 (AltMin-CG).

4. Convergence analysis. In this section, we will show the global convergence of Algorithm 1 (AltMin) to a critical point. It will come as a consequence of the results in [53, section 2].

4.1. Preliminaries. The following definitions and lemmas ([45], [3, Definition 1]) are used for the convergence analysis in the next subsection.

DEFINITION 4.1. Let $f : \mathbb{R}^m \mapsto \mathbb{R} \cup \{+\infty\}$ be proper and lower semicontinuous. (i) The domain of f is defined and denoted by $\text{dom} f := \{\mathbf{x} \in \mathbb{R}^m : f(\mathbf{x}) < +\infty\}$. (ii) For each $\mathbf{x} \in \text{dom} f$, the Fréchet subdifferential of f at \mathbf{x} , denoted as $\hat{\partial}f(\mathbf{x})$, is defined as follows:

$$\hat{\partial}f(\mathbf{x}) = \left\{ \xi \in \mathbb{R}^m : \liminf_{\substack{\mathbf{y} \neq \mathbf{x} \\ \mathbf{y} \rightarrow \mathbf{x}}} \frac{f(\mathbf{y}) - f(\mathbf{x}) - \langle \xi, \mathbf{x} - \mathbf{y} \rangle}{\|\mathbf{x} - \mathbf{y}\|} \geq 0 \right\}.$$

If $\mathbf{x} \notin \text{dom} f$, then $\hat{\partial}f(\mathbf{x}) = \emptyset$. (iii) The limiting subdifferential of f at $\mathbf{x} \in \text{dom} f$, denoted as $\partial f(\mathbf{x})$, is defined as follows [36]

$$\partial f(\mathbf{x}) := \{\xi^* \in \mathbb{R}^m : \exists (\mathbf{x}_n)_{n \geq 0}, \mathbf{x}_n \rightarrow \mathbf{x}, f(\mathbf{x}_n) \rightarrow f(\mathbf{x}), \text{ s.t. } \exists \xi_n \in \hat{\partial}f(\mathbf{x}_n), \xi_n \rightarrow \xi^*\}.$$

DEFINITION 4.2 (KL function [53, Definition 2.5]). A function $f(\mathbf{x})$ satisfies the Kurdyka-Łojasiewicz (KL) property at point $\bar{\mathbf{x}} \in \text{dom}(\partial f)$ if, in a certain neighborhood \mathcal{U} of $\bar{\mathbf{x}}$, there exists $\psi(s) = cs^{1-\theta}$ for some $c > 0$ and $\theta \in [0, 1)$ such that the KL inequality below holds:

$$\psi'(f(\mathbf{x}) - f(\mathbf{x}^*)) \text{dist}(0, \partial f(\mathbf{x})) \geq 1, \text{ for any } \mathbf{x} \in \mathcal{U} \cap \text{dom}(\partial f) \text{ and } f(\mathbf{x}) \neq f(\mathbf{x}^*),$$

where $\text{dom}(\partial f) = \{\mathbf{x} : \partial f(\mathbf{x}) \neq \emptyset\}$ and $\text{dist}(0, \partial f(\mathbf{x})) = \min\{\|\mathbf{y}\| : \mathbf{y} \in \partial f(\mathbf{x})\}$.

If f satisfies the KL property at each point of $\text{dom}(f)$, f is called a KL function.

DEFINITION 4.3 (Strong convexity). A differentiable function $f : \text{dom} f \mapsto \mathbb{R}$ is strongly convex if and only if

$$f(\mathbf{y}) \geq f(\mathbf{x}) + \langle \nabla f(\mathbf{x}), \mathbf{y} - \mathbf{x} \rangle + \frac{\mu}{2} \|\mathbf{y} - \mathbf{x}\|^2$$

holds for some $\mu > 0$ and all $\mathbf{x}, \mathbf{y} \in \text{dom} f$.

DEFINITION 4.4 (Coercivity). A real-valued function $f : \mathbb{R}^m \rightarrow \mathbb{R}$ is called coercive if and only if $f(\mathbf{x}) \rightarrow +\infty$ as $\|\mathbf{x}\| \rightarrow +\infty$.

4.2. Convergence properties of AltMin. The following two lemmas follow directly from Theorem 2.8 and Theorem 2.9 of [53] and are used for proving the convergence of the proposed alternating minimization method.

LEMMA 4.5. Assume f satisfies the KL property and ∇f is Lipschitz continuous on any bounded subset of its domain. Let $(U_0^{(1)}, \dots, U_0^{(k)})$ be any initialization and $(U_t^{(1)}, \dots, U_t^{(k)})$ be the sequence generated by Algorithm 1, where each subproblem $f_t^{(i)}(U^{(i)})$ (line 7 of Algorithm 1) is strongly convex and is solved exactly. If the sequence $(U_t^{(1)}, \dots, U_t^{(k)})$ is bounded and there exists a finite limit point $(U_*^{(1)}, \dots, U_*^{(k)})$, then it converges to $(U_*^{(1)}, \dots, U_*^{(k)})$, which is a critical point of f .

The convergence rate of the sequence is as follows.

LEMMA 4.6. Assume ∇f is Lipschitz continuous on any bounded set and suppose that $U_t^{(i)}$ converges to a critical point $U_*^{(i)}$ for $i = 1, \dots, k$, at which f satisfies the KL inequality with $\psi(s) = cs^{1-\theta}$ for $c > 0$ and $\theta \in [0, 1)$. We have:

1. If $\theta = 0$, $U_t^{(i)}$ converges to $U_*^{(i)}$ in a finite number of iterations;
2. If $\theta \in (0, \frac{1}{2}]$, $\|U_t^{(i)} - U_*^{(i)}\| \leq \beta \tau^t$, $\forall t \geq t_0$ for certain $t_0 > 0$, $\beta > 0$, $\tau \in [0, 1)$;
3. If $\theta \in (\frac{1}{2}, 1)$, $\|U_t^{(i)} - U_*^{(i)}\| \leq \beta t^{-(1-\theta)/(2\theta-1)}$, $\forall t \geq t_0$ for certain $t_0 > 0$, $\beta > 0$.

Part 1, 2 and 3 correspond to finite convergence, linear convergence, and sublinear convergence, respectively.

We show that the iterates generated by Algorithm 1 (AltMin) converge to a stationary point in the following theorem. Note that this theorem applies to Algorithm 2 (AltMin-CG), provided that the updated

iterate of each of the subproblems (line 8 in Algorithm 2) is the exact minimizer of the corresponding (graph-regularized) least-squares problem. In practice, this requires setting a sufficiently low tolerance parameter ϵ for the subproblem solver (Algorithm 3).

THEOREM 4.7. *The iterates $(U_t^{(1)}, \dots, U_t^{(k)})$ generated by Algorithm 1 (AltMin) from any initialization converge globally to a critical point of f in (2.4). Moreover, linear convergence and sublinear convergence in parts 2 and 3 of Lemma 4.6 apply depending on θ in KL property of f .*

Proof. According to Lemma 4.5, we need to check whether all the assumptions satisfied.

1) Function f in (2.4) is a KL function with $\theta \in [1/2, 1)$ as it is a combination of polynomials which are one kind of real analytic functions (see [27, Definition 1.1.5]). The real analytic function itself and the finite sum or product of real analytic functions are KL functions, see [3, section 4] and [53, section 2.2].

2) Gradient ∇f is Lipschitz continuous on any bounded subset of domain since f is a C^∞ function.

3) For $i = 1, \dots, k$, $f^{(i)}$ in (3.2) is strongly convex by Definition 4.3 since $L^{(i)}$ in (2.5) is positive definite. Therefore, the quadratic form $g^{(i)}$ of the subproblems (3.3) is strongly convex through the identification $g^{(i)}(\text{vec}((U^{(i)})^\top)) = f^{(i)}(U^{(i)})$. Moreover, the solution for each $g^{(i)}$ corresponds to the exact minimizer.

4) Notice that since f is coercive as defined in Definition 4.4 and real analytic, it is guaranteed to produce a bounded sequence $(U_t^{(1)}, \dots, U_t^{(k)})$, thus it has a critical point $(U_*^{(1)}, \dots, U_*^{(k)})$.

Lemma 4.5 then implies that the sequence generated by Algorithm 2 from any initial point converges to a critical point $(U_*^{(1)}, \dots, U_*^{(k)})$ of f . Moreover, the asymptotic convergence rates in parts 2 and 3 of Lemma 4.6 apply as $\theta \in [1/2, 1)$. \square

5. Experiments. In this section, we carry out some numerical experiments to demonstrate the workings of our proposed algorithms Algorithm 2 (AltMin-CG) and Algorithm 5 (ADMM) on the LRTC model (2.4). All numerical experiments were performed on a Macbook Pro with a 2.3 GHz Intel Core i7 CPU, 16GB RAM and MATLAB R2015a with Tensor Toolbox version 2.5 [4]. The source code is made available online.²

First, we test the effect of the graph Laplacian regularization in the LRTC model (2.4) and we compare the recovery quality of solutions to the graph-regularized tensor completion model to two other models without graph regularization. Then, we evaluate time efficiency of the proposed methods (Algorithm 2 and Algorithm 5) in optimizing the graph-regularized model (2.4), and compare them with the baseline methods on both synthetic data and real data.

5.1. Experimental methodology and datasets. In the experiments, we evaluate the recovery performance of a tensor completion result $\hat{\mathcal{T}} := \llbracket U^{(1)}, \dots, U^{(k)} \rrbracket$ with the following error functions restricted on an index set Ω' —which contains the revealed entries or the unrevealed entries for test error—of \mathcal{T} : (i) the relative error of $\hat{\mathcal{T}}$ against \mathcal{T} in the Frobenius norm, and (ii) the root mean squared error (RMSE) of $\hat{\mathcal{T}}$. The training and test RMSEs refer to the RMSE on the training set (Ω_{tr})—the set of revealed entries for the optimization of the model—and the test set respectively.

We initialize both our proposed methods and other methods with a point $U_0 \in \mathbb{R}^{m_1 \times R} \times \mathbb{R}^{m_2 \times R} \times \mathbb{R}^{m_3 \times R}$ where each factor matrix $U_0^{(i)}$ is a Gaussian matrix such that $[U_0^{(i)}]_{jr} \sim \mathcal{N}(0, 1)$.

The stopping criterion in Algorithm 1 (line 3) is satisfied if either of the following conditions is met: (i) the wall time used for producing the latest iterate is larger than a time budget parameter T_{max} ; (ii) the progress of the iterate $(U_t^{(i)})_{i=1, \dots, k}$, measured by a heuristic difference function Δ_t , is smaller than a tolerance parameter ϵ . Here we define Δ_t as follows,

$$\Delta_t := |E(U_t; \Omega_{\text{tr}}) - E(U_{t-1}; \Omega_{\text{tr}})| \quad \text{with} \quad E(U; \Omega_{\text{tr}}) := \frac{\|P_{\Omega_{\text{tr}}}(\llbracket U^{(1)}, \dots, U^{(k)} \rrbracket - \mathcal{T})\|_{\text{F}}}{\|P_{\Omega_{\text{tr}}}(\mathcal{T})\|_{\text{F}}}, \quad (5.1)$$

where $E(U; \Omega_{\text{tr}})$ is the relative error restricted on the training set Ω_{tr} .

Based on a ground truth tensor $\mathcal{T} \in \mathbb{R}^{m_1 \times m_2 \times m_3}$ and for a fixed sampling rate, we generate N_{test} training instances $(\Omega_\ell)_{\ell=1, \dots, N_{\text{test}}}$ under the same sampling rate. For each training instance $(\mathcal{T}, \Omega_\ell)$, N_{init} initial points

²<https://gitlab.com/ricky7guanyu/tensor-completion-with-regularization-term>

$(U_{0,(\ell,j)})$, for $j = 1, \dots, N_{\text{init}}$, are generated. Let $\hat{\mathcal{T}}(U_{0,(\ell,j)}; \Omega_\ell)$ denote the solution of the j -th test based on the training instance $(\mathcal{T}, \Omega_\ell)$ with the initial point $U_{0,(\ell,j)}$, and $E(\hat{\mathcal{T}})$ the error (e.g., relative error, RMSE) of the candidate tensor $\hat{\mathcal{T}}$ w.r.t. \mathcal{T} . Then each method is evaluated by the following score

$$\bar{E}(\hat{\mathcal{T}}) = \frac{1}{N_{\text{test}} N_{\text{init}}} \sum_{\ell=1}^{N_{\text{test}}} \sum_{j=1}^{N_{\text{init}}} E(\hat{\mathcal{T}}(U_{0,(\ell,j)}; \Omega_\ell)).$$

In all experiments we set $N_{\text{test}} = 5$ and $N_{\text{init}} = 10$.

In all experiments, the problem-related parameters (λ_i, λ_L) in (2.4)–(2.5) are generated randomly with the uniform distribution in the log scale. Then the parameter is chosen among all generated parameter settings through K -fold cross validation (for $K = 3$).

Synthetic data. To investigate the effects of graph regularization in the tensor completion model (2.4), it is tempting to generate a synthetic low rank tensor \mathcal{T} that can be related to structural information of a certain graph. For this purpose, we consider the following tensor model. First, we generate k Gaussian matrices $(U^{(1)}, \dots, U^{(k)})$ of size $m_i \times R$, for a rank parameter $0 < R < \min(m_i)$. Then, we generate a graph Laplacian matrix $\mathcal{L}^{(1)}$ on the row index set of $U^{(1)}$ from the ‘‘Community’’ graph model (a type of graphs that contain a number of different closely connected subgraphs or clusters) of GSPbox [41]. The structural information of the graph Laplacian is obtained through the eigenvalue value decomposition $\mathcal{L}^{(i)} := \mathcal{U}\Lambda\mathcal{U}^\top$, and is affected to the final tensor model as follows

$$\mathcal{T} := \llbracket \tilde{U}^{(1)}, U^{(2)}, \dots, U^{(k)} \rrbracket + \mathcal{E} \quad \text{for} \quad \tilde{U}^{(1)} := \mathcal{U}\Lambda^{-1}U^{(1)}, \quad (5.2)$$

where \mathcal{E} represents a tensor containing additive noise such that $\mathcal{E}_{\ell_1 \ell_2 \ell_3} \sim \mathcal{N}(0, \sigma)$, where σ is set by a given signal-to-noise ratio (SNR). In the experiments, the SNR is set as 20 dB.

The tensor model (5.2), in the same spirit as the synthetic matrix model in [42, 18], has the effect of creating pairwise similar entries (along the first dimension) according to the graph connections. In fact, the columns of $\tilde{U}^{(1)} = \mathcal{U}\Lambda^{-1}U^{(1)}$, by construction, belong to the eigensubspace of the given graph Laplacian matrix $\mathcal{L}^{(1)}$ with a prescribed order of weights in the direction of each eigenvector; here the weights are given by $(\Lambda_{ii}^{-1})_{i=1, \dots, m_1}$ which make the eigenvectors with the lowest eigenvalues the most significant components of $\tilde{U}^{(1)}$. Therefore, based on graph spectral analysis, each column of $\tilde{U}^{(1)}$ is a smooth-varying function on the given graph.

In the experiments third-order tensors are tested with dimensions set as $(m_1, \dots, m_3) = (100, 100, 100)$, and the rank parameter in (5.2) is set as $R = 10$.

MovieLens dataset. The MovieLens-100k dataset³ consists of 100,000 movie ratings from 943 users on 1682 movies during a seven-month period from September 19th, 1997 through April 22nd, 1998. Each movie rating in this dataset has a time stamp. Therefore, we obtain a tensor \mathcal{T} of size $943 \times 1682 \times 7$ (i.e., time period is split into 7 parts). We randomly select 80% of the known ratings as training set.

FIA dataset. In this experiment, we use the ‘‘rank-deficient spectral FIA dataset’’.⁴ This dataset consists of results of flow injection analysis on 12 different chemical substances. The represented tensor is of size 12 (substances) \times 100 (wavelengths) \times 89 (reaction times).

5.2. Graph-regularized tensor completion. In this subsection, we evaluate the graph-regularized tensor completion model in comparison to models without graph Laplacian regularization. Hereafter, we label the graph Laplacian regularizer of the tensor completion model (2.4) as GraphReg, which also denotes by abuse the model (2.4) with $\lambda_i \neq 0$ and $\lambda_L \neq 0$. The Frobenius norm-based regularizers in (2.4) is labeled as FrobReg, which denotes the tensor completion model (2.4) when the graph Laplacian regularizer is reduced to zero, i.e., $\lambda_L = 0$ while the other regularizers are active ($\lambda_i \neq 0$). The unregularized model, i.e., (2.4) when all regularization parameters $\lambda_i = \lambda_L = 0$, is labeled as Unregularized. In the experiments of this subsection, the

³<https://grouplens.org/datasets/movielens/100k/>

⁴<http://www.models.life.ku.dk/datasets>

stopping criterion is controlled by (i) a large enough iteration budget T_{\max} ; and (ii) a global tolerance parameter ϵ for (5.1).

Experiment on synthetic data. In this experiment, we consider tensors generated from the synthetic model (5.2), which incorporates the graph Laplacian information of a given graph. We conduct tensor completion tests for different sampling rates in $\{0.3\%, 0.5\%, 0.7\%, 1\%\}$. The rank parameter for all LRTC models is set as $R = 10$. The average relative errors are listed in Table 5.1. Figure 5.1 shows the histogram with $SR = 0.3\%$. We see that in this experiment where AltMin-CG and ADMM are used, the GraphReg model outperforms the other two models.

TABLE 5.1

Average recovery accuracy (relative error) of the three tensor completion models on synthetic data: GraphReg (with graph Laplacian), FroReg (without graph Laplacian), Unregularized (no regularizer).

Sampling Rate	Algorithm	GraphReg	FrobReg	Unregularized
0.3%	AltMin-CG	0.8198	1.0083	7.1110
	ADMM	0.8246	1.0054	4.4393
0.5%	AltMin-CG	0.4418	0.9201	9.9010
	ADMM	0.4486	0.9236	7.6692
0.7%	AltMin-CG	0.3106	0.7561	9.9548
	ADMM	0.3000	0.7487	8.4821
1%	AltMin-CG	0.1380	0.4772	13.5740
	ADMM	0.1439	0.4513	10.9230

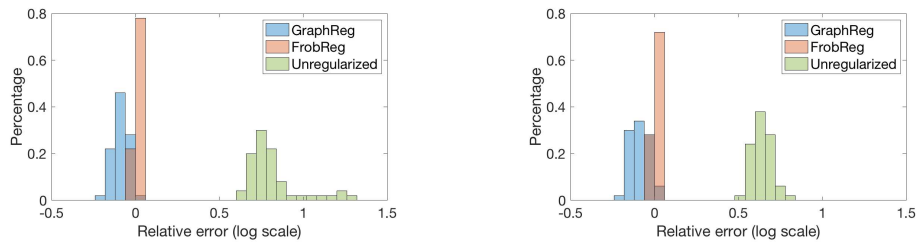


FIGURE 5.1. Histogram of recovery errors of the three tensor completion models on synthetic data. The sampling rate is 0.3%. (Left) AltMin-CG; (Right) ADMM.

Experiment on the MovieLens dataset. Next, we conduct the same experiment on the MovieLens dataset. An essential difference with the previous experiment on synthetic data is that the desired similarity graph for regularizing the tensor completion model is not directly available but requires either a collection of auxiliary graph information or construction from data with a certain graph model.

In the case of the MovieLens dataset, we assume the similarity patterns among the revealed data entries already contains information for constructing a similarity graph on the set of users or the set of items. The reasoning is that for a pair of users that have already given the same (or similar) scores on a same subset of movies, then it is likely that they have similar preferences, and hence they are supposed to be connected for a user-similarity graph. The similar argument applies to pairs of movies that have very close ratings from users. Therefore, we construct a movie-wise similarity graph based on the data matrix itself (with missing

entries). Let M^* denote the MovieLens data matrix with missing entries. We compute the graph proximity parameters based on a low-rank approximation of the partially revealed matrix. More precisely, we use a rank- r approximation of the zero-filled matrix $M_0 := P_\Omega(M^*) \in \mathbb{R}^{m \times n}$ as the features for constructing the graph. Let (U_0, S_0, V_0) denote the r -SVD of M_0 and let $\widetilde{M}_0 := U_0 S_0 V_0^T$.

Next, the computation of the graph edge weight parameters based on the given matrix $M := \widetilde{M}_0$ can be realized using various node proximity methods such as K -Nearest Neighbors (K -NN) and ε -graph models [12, 6, 23, 13], which boil down to computing a certain distance matrix between the rows (resp. columns) of M . Let $Z^r(M) \in \mathbb{R}^{m \times m}$ denote the row-wise distance matrix of M defined as $Z_{ij}(M) = \text{dist}(M_{i,:}, M_{j,:})$, for $i, j \in [m]$, where $\text{dist} : \mathbb{R}^n \times \mathbb{R}^n \mapsto \mathbb{R}_+$ is a distance on the n -dimensional vector space. Subsequently, we build a Gaussian ε -graph by computing the node proximity weights as follows

$$(W_\varepsilon(M))_{ij} = \exp(-\varepsilon^{-2}Z_{ij}(M)) \quad \text{for } i, j \in [m] \quad (5.3)$$

where $\varepsilon \in \mathbb{R}$ is a hyperparameter of the graph model. Furthermore, a sparse graph adjacency matrix is preferable to a dense one from a computational point of view, as the per-iteration cost of the proposed algorithms (e.g. Algorithm 2) depends partly on $\text{nnz}(L^r)$ and $\text{nnz}(L^c)$. For simplicity, we sparsify the graph adjacency matrix defined in (5.3) with the following thresholding operation

$$(W_{\varepsilon, \sigma}(M))_{ij} = \mathbf{1}_{\geq \sigma}(\exp(-\varepsilon^{-2}Z_{ij}(M))) \quad \text{for } i, j \in [m], \quad (5.4)$$

where $\mathbf{1}_{\geq \sigma}$ is the hard threshold function such that $\mathbf{1}_{\geq \sigma}(z) = z$ if $z \geq \sigma$ and 0 otherwise. In the graph model (5.4), parameter ε is tuned according to the variance of $(Z_{ij})_{i,j=1,\dots,m}$ and threshold σ is chosen according to a preset sparsity level $\varepsilon \ll 1$ for the edge set associated with $W_{\varepsilon, \sigma}$ such that $\frac{|\mathcal{E}(W_{\varepsilon, \sigma})|}{m^2} \leq \varepsilon$.

The rank parameter for all three LRTC models (GraphReg, FrobReg and Unregularized) is set as $R = 10$. The results are given in Table 5.2 and the histogram of these results is presented in Figure 5.2. These results show that the solutions to the graph-regularized model (2.4) (labeled GraphReg) and FrobReg model have better recovery performance (in terms of RMSE) than Unregularized model. The gain of recovery performance induced by the graph learned from the data may be considered marginal; however, on movie rating data, it is notoriously difficult to improve the RMSE score much beyond basic methods [7].

TABLE 5.2

Relative error of the three models on the MovieLens dataset: GraphReg (with graph Laplacian), FrobReg (without graph Laplacian), Unregularized (no regularizer).

Algorithm	GraphReg	FrobReg	Unregularized
AltMin-CG	0.2233	0.2233	1.4526
ADMM	0.2193	0.2234	1.1205

Experiment on the FIA dataset. For the graph Laplacian regularization, we construct the adjacency matrices following the ideas in [38, Section 4.1].⁵ For 12 chemical substances, we build the adjacency matrix with edge weights defined from the inverse of the Euclidean distance of the corresponding pairs of feature vectors. Along the index set of wavelengths and reaction times, respectively, we construct an adjacency matrix using the chain graph model, which models the connectivity of neighboring wavelengths or time stamps, since the observations on the chemical substances generally vary smoothly in the domain of wavelengths and also in time.

The sampling rate varies among 1%, 5% and 7%. We present in Table 5.3 average relative errors after running 50 random tests, and in Figure 5.3 the histogram of relative errors under the sampling rate 1%. Similar to the comparative results on synthetic data, these results show that the solutions of the GraphReg model have smaller recovery errors compared to those of the other two models.

⁵A comparison between the proposed methods and the TFAI method of [38] is made; see Section 5.3.

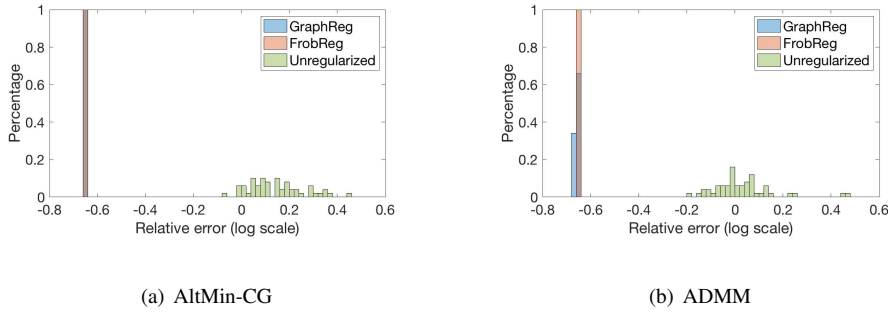


FIGURE 5.2. Histogram of recovery errors of the three tensor completion models on the MovieLens dataset.

TABLE 5.3

Relative error of the three models on the FIA dataset: GraphReg (with graph Laplacian), FrobReg (without graph Laplacian), Unregularized (no regularizer).

Sampling rate	Algorithm	GraphReg	FrobReg	Unregularized
1%	AltMin-CG	0.1012	1.1096	6.6597
	ADMM	0.2396	1.1385	1.5985
5%	AltMin-CG	0.0146	0.3470	3.9619
	ADMM	0.0209	0.2131	0.2131
7%	AltMin-CG	0.0126	0.2087	0.3837
	ADMM	0.0180	0.0572	0.0572

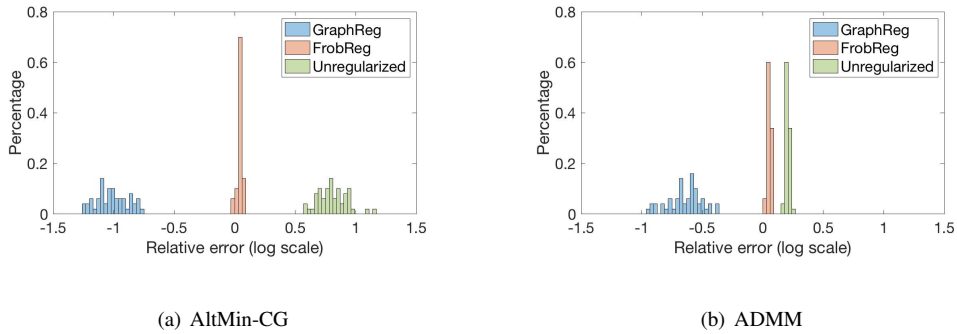


FIGURE 5.3. Histogram of recovery errors of the three tensor completion models on the FIA dataset. The sampling rate is 1%.

Observations and results. From the results on the real-world datasets, the graph-regularized model (2.4) (GraphReg) shows improvements in the recovery accuracy on both the MovieLens and the FIA datasets. Especially with the FIA dataset, the improvements by GraphReg is increasingly significant when the sampling rate decreases from 7% to 1%. A possible explanation is that the graphs constructed for the FIA dataset are good enough in capturing the entrywise similarities in the (partially observed) tensor while in the case of MovieLens, the graph constructed (using the model (5.4)) is less adapted to the real-world user/movie similarities.

Similarly and even more evidently, the results (Table 5.1) on synthetic datasets (for which the graph information is given) show that the graph-regularized model (2.4) entails significant improvements over the other two models without graph regularization, under all sampling rates tested. This observation validates the improvements by the GraphReg model for tensor completion especially when the proportion of the revealed entries (the sampling rate) is low.

5.3. Time efficiency evaluations. In this subsection, we focus on evaluating the time efficiency of our proposed algorithms under the same experimental settings described in the last subsection. In each of the following experiments, iteration information for our proposed algorithms is recorded. At each iteration, the recovery quality of the current iterate is evaluated in terms of the RMSE on test entries.

Besides our proposed algorithms, the state-of-art methods mentioned in Section 2.2 are also tested using implementations that are publicly available or made available to us: (i) INDAFAC, the damped Gauss-Newton method proposed by Tomasi and Bro [50]; (ii) CP-WOPT, a CP decomposition algorithm by Acar et al [1] which is available in the Tensor Toolbox [4]; (iii) BPTF, a Bayesian probabilistic tensor CPD algorithm [52]; (iv) TFAI, an algorithm for tensor factorization with the within-mode auxiliary information; (v) TNCP, an ADMM algorithm for solving a matrix trace-norm regularized model [34]; and (vi) AirCP, an ADMM algorithm for solving the CP-based tensor completion using auxiliary graph information [22]. The parameters involved in the models of TFAI, TNCP and AirCP are chosen after cross validation.

Experiment on synthetic data. Under the same experimental settings as for Table 5.1, the RMSEs of the iterates given by the tested methods are shown in Figure 5.4. The iterative results in the figures are taken from one test randomly chosen from the repeated tests. Figure 5.4 shows the results under the sampling rates 0.3% and 0.5%, in which we observe that proposed algorithms, AltMin-CG and ADMM, have a better time efficiency than in Section 5.3.

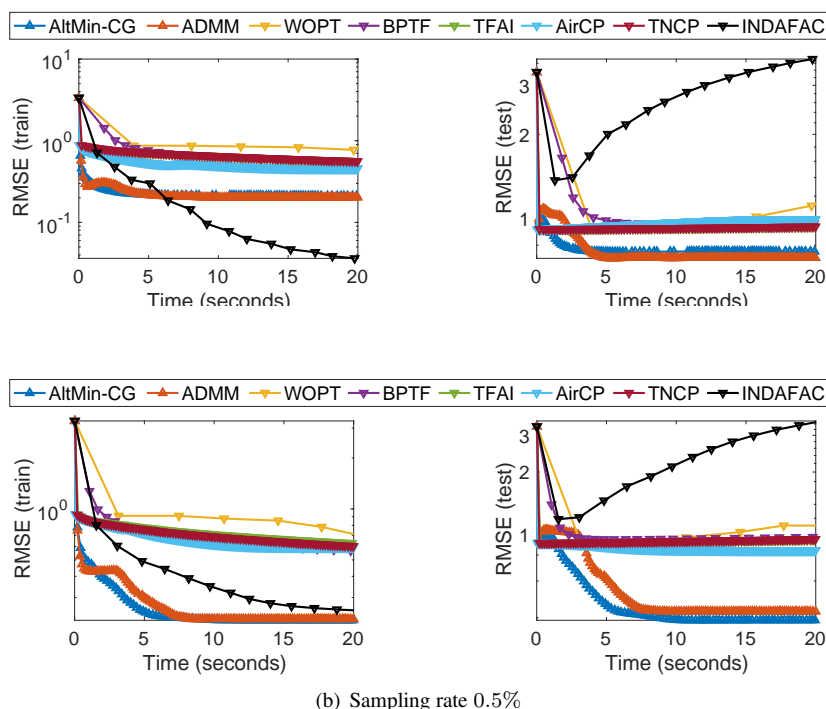


FIGURE 5.4. Iterative results of the tested algorithms on synthetic data: RMSE on training and test sets by accumulative time per iteration. The sampling rates are 0.3% and 0.5%.

Experiment on MovieLens. Under the same experimental settings on the MovieLens dataset and with the same graph construction method as in the previous subsection, we show the RMSEs of the iterates given by the tested methods in Figure 5.5. The iterative results in the figure are taken from one test randomly chosen from the repeated tests. In particular, the labels “AltMin-CG1” and “ADMM1” represent the results of these algorithms under the graph-agnostic, nuclear norm-based model (NuclReg-TC). The results therein shows that the AltMin-CG and ADMM methods remain competitive on this dataset, in particular their time efficiency is comparable

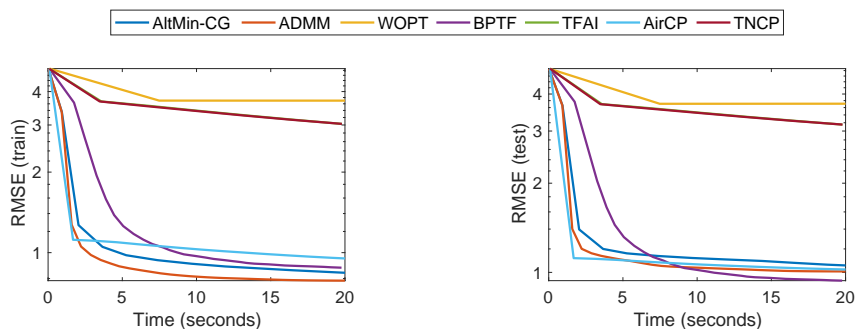
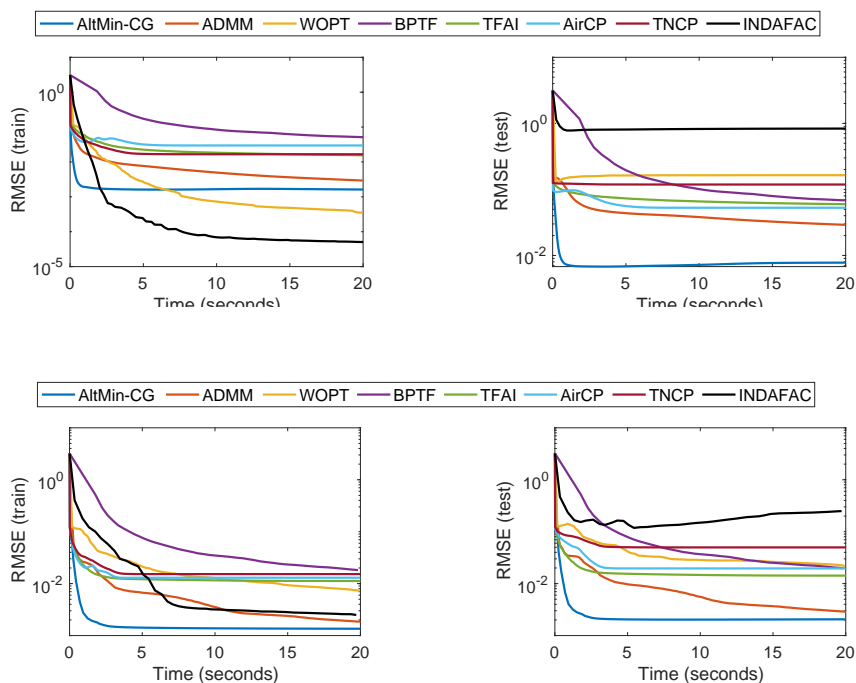


FIGURE 5.5. Iterative results of the tested algorithms on the MovieLens dataset: RMSE on training and test sets by accumulative time per-iteration.



(b) Sampling rate 5.0%

FIGURE 5.6. Iterative results of the tested algorithms on the FIA dataset: RMSE on training and test sets by accumulative time per-iteration.

Experiment on the FIA dataset. Under the same experimental settings on the FIA dataset and with the same graph construction method as in the previous subsection, we show the RMSEs of the iterates given by

the tested methods in Figure 5.6. The iterative results in the figure are taken from one test randomly chosen from the repeated tests. These results show that the proposed algorithms AltMin-CG and ADMM yield the best recovery performances (in terms of test RMSE).

Observations and results. From Figure 5.4, we observe that most of the methods perform comparably in time efficiency. In particular, the proposed AltMin-CG and ADMM methods, followed by AirCP, TFAI, TNCP, are the fastest in terms of training RMSE. Also, AltMin-CG and ADMM achieve the lowest test RMSEs, under low sampling rates. This result is encouraging since it shows that our methods and model for tensor completion can achieve robust recovery where only a small fraction of data is available.

For real data in Figure 5.5, AirCP, TFAI, AltMin-CG and ADMM have comparable time efficiencies and are the fastest among all tested algorithms in terms of training error. BPTF is slower than the aforementioned methods but obtains the lowest test RMSE. In Figure 5.6, we also observe that the proposed AltMin-CG and ADMM methods outperform most other methods both in efficiency and accuracy with the given training data that correspond to low sampling rates.

6. Conclusion. In this paper, we studied a CP decomposition-based tensor completion model (2.4) that involves graph regularization. This model is motivated by two main reasons: (i) the CP decomposition enables a memory-efficient model for low-rank tensors and (ii) the use of the graph Laplacian-based regularizer is shown to be effective in many tasks such as semi-supervised learning, image restoration and also matrix completion, which makes graph regularization a tempting tool for tensor completion. For the optimization of this completion model of k -th order tensors, we proposed an alternating minimization algorithm and an ADMM algorithm adapted to the block structure of the underlying problem. Within the alternating minimization procedure, we showed that each of the k subproblems is a quadratic minimization problem, and we adapted a linear CG method for solving these subproblems. An efficient Hessian-vector multiplication was used for the linear CG subroutine. Besides, we proposed an ADMM algorithm, which further resolves an undesirable coupling effect of graph regularization on the optimization of the problem. The convergence property of the proposed AltMin algorithm was analysed.

From the results of various numerical experiments, we verified that the graph-regularized tensor completion model (2.4) produces improved tensor completion results with respect to tensor completion models without graph regularization. This observation is especially significant when the sample rate is small. The proposed algorithms, AltMin-CG (Algorithm 2) and ADMM (Algorithm 5), have also shown to have superior or comparable completion results with improved time efficiency at the same time, compared to state-of-art methods.

Acknowledgement. This work was supported by the Fonds de la Recherche Scientifique – FNRS and the Fonds Wetenschappelijk Onderzoek – Vlaanderen under EOS Project no. 30468160 (SeLMA – Structured low-rank matrix/tensor approximation: numerical optimization-based algorithms and applications) and by the Fonds de la Recherche Scientifique – FNRS under Grant no. T.0001.23. The second author was supported by the FNRS through a FRIA scholarship. The third author was supported by the Young Elite Scientist Sponsorship Program by CAST.

REFERENCES

- [1] EVRIM ACAR, DANIEL M DUNLAVY, TAMARA G KOLDA, AND MORTEN MØRUP, *Scalable tensor factorizations for incomplete data*, Chemometrics and Intelligent Laboratory Systems, 106 (2011), pp. 41–56.
- [2] RIE ANDO AND TONG ZHANG, *Learning on graph with Laplacian regularization*, Advances in neural information processing systems, 19 (2006).
- [3] HÉDY ATTOUCH, JÉRÔME BOLTE, PATRICK REDONT, AND ANTOINE SOUBEYRAN, *Proximal alternating minimization and projection methods for nonconvex problems: An approach based on the Kurdyka-Lojasiewicz inequality*, Mathematics of Operations Research, 35 (2010), pp. 438–457.
- [4] BRETT W BADER, TAMARA G KOLDA, ET AL., *Tensor Toolbox for MATLAB, version 2.5, 2012*.
- [5] DANIEL BANCO, SHUCHIN AERON, AND W SCOTT HOGE, *Sampling and recovery of MRI data using low rank tensor models*, in 2016 38th Annual International Conference of the IEEE Engineering in Medicine and Biology Society (EMBC), IEEE, 2016, pp. 448–452.

- [6] MIKHAIL BELKIN AND PARTHA NIYOGI, *Laplacian eigenmaps for dimensionality reduction and data representation*, Neural computation, 15 (2003), pp. 1373–1396.
- [7] JAMES BENNETT, STAN LANNING, ET AL., *The Netflix prize*, in Proceedings of KDD cup and workshop, vol. 2007, Citeseer, 2007, p. 35.
- [8] MARCELO BERTALMIO, GUILLERMO SAPIRO, VINCENT CASELLES, AND COLOMA BALLESTER, *Image inpainting*, in Proceedings of the 27th annual conference on Computer graphics and interactive techniques, ACM Press/Addison-Wesley Publishing Co., 2000, pp. 417–424.
- [9] STEPHEN BOYD, NEAL PARIKH, ERIC CHU, BORJA PELEATO, JONATHAN ECKSTEIN, ET AL., *Distributed optimization and statistical learning via the alternating direction method of multipliers*, Foundations and Trends® in Machine learning, 3 (2011), pp. 1–122.
- [10] JIAN-FENG CAI, WEN HUANG, HAIFENG WANG, AND KE WEI, *Tensor completion via tensor train based low-rank quotient geometry under a preconditioned metric*, arXiv preprint arXiv:2209.04786, (2022).
- [11] EMMANUEL J CANDÈS AND BENJAMIN RECHT, *Exact matrix completion via convex optimization*, Foundations of Computational mathematics, 9 (2009), p. 717.
- [12] BERNARD CHAZELLE, *An improved algorithm for the fixed-radius neighbor problem*, Information Processing Letters, 16 (1983), pp. 193–198.
- [13] JIE CHEN, HRFANG@MCS ANL GOV, AND YOUSEF SAAD, *Fast Approximate kNN Graph Construction for High Dimensional Data via Recursive Lanczos Bisection* *Haw-ren Fang*, Journal of Machine Learning Research, 10 (2009).
- [14] GENE CHEUNG, ENRICO MAGLI, YUICHI TANAKA, AND MICHAEL K NG, *Graph spectral image processing*, Proceedings of the IEEE, 106 (2018), pp. 907–930.
- [15] FAN RK CHUNG AND FAN CHUNG GRAHAM, *Spectral graph theory*, no. 92, American Mathematical Soc., 1997.
- [16] RONALD R COIFMAN, STEPHANE LAFON, ANN B LEE, MAURO MAGGIONI, BOAZ NADLER, FREDERICK WARNER, AND STEVEN W ZUCKER, *Geometric diffusions as a tool for harmonic analysis and structure definition of data: Diffusion maps*, Proceedings of the national academy of sciences, 102 (2005), pp. 7426–7431.
- [17] CURT DA SILVA AND FJ HERRMANN, *Hierarchical tucker tensor optimization-applications to tensor completion. SampTA 2013*, in 10th International Conference on Sampling Theory and Application, Jacobs University Bremen, 2013.
- [18] SHUYU DONG, P-A ABSIL, AND KA GALLIVAN, *Riemannian gradient descent methods for graph-regularized matrix completion*, Linear Algebra and its Applications, 623 (2021), pp. 193–235.
- [19] SHUYU DONG, BIN GAO, YU GUAN, AND FRANÇOIS GLINEUR, *New Riemannian preconditioned algorithms for tensor completion via polyadic decomposition*, SIAM Journal on Matrix Analysis and Applications, 43 (2022), pp. 840–866.
- [20] SILVIA GANDY, BENJAMIN RECHT, AND ISAO YAMADA, *Tensor completion and low-n-rank tensor recovery via convex optimization*, Inverse Problems, 27 (2011), p. 025010.
- [21] BIN GAO, RENFENG PENG, AND YA-XIANG YUAN, *Riemannian preconditioned algorithms for tensor completion via tensor ring decomposition*, arXiv preprint arXiv:2302.14456, (2023).
- [22] HANCHENG GE, JAMES CAVERLEE, NAN ZHANG, AND ANNA SQUICCIARINI, *Uncovering the spatio-temporal dynamics of memes in the presence of incomplete information*, in Proceedings of the 25th ACM International on Conference on Information and Knowledge Management, ACM, 2016, pp. 1493–1502.
- [23] XIAOFEI HE AND PARTHA NIYOGI, *Locality preserving projections*, in Advances in neural information processing systems, 2004, pp. 153–160.
- [24] FRANK L HITCHCOCK, *The expression of a tensor or a polyadic as a sum of products*, Journal of Mathematics and Physics, 6 (1927), pp. 164–189.
- [25] PRATEEK JAIN AND SEWOONG OH, *Provable tensor factorization with missing data*, Advances in Neural Information Processing Systems, 27 (2014).
- [26] TAMARA G. KOLDA AND BRETT W. BADER, *Tensor decompositions and applications*, SIAM Rev., 51 (2009), pp. 455–500.
- [27] STEVEN G KRANTZ AND HAROLD R PARKS, *A primer of real analytic functions*, Springer Science & Business Media, 2002.
- [28] JOSEPH B KRUSKAL, *Three-way arrays: rank and uniqueness of trilinear decompositions, with application to arithmetic complexity and statistics*, Linear algebra and its applications, 18 (1977), pp. 95–138.
- [29] TIMOTHÉE LACROIX, NICOLAS USUNIER, AND GUILLAUME OBOZINSKI, *Canonical tensor decomposition for knowledge base completion*, in International Conference on Machine Learning, PMLR, 2018, pp. 2863–2872.
- [30] SHIYONG LAN, YITONG MA, WEIKANG HUANG, WENWU WANG, HONGYU YANG, AND PYANG LI, *DSTAGNN: Dynamic spatial-temporal aware graph neural network for traffic flow forecasting*, in International conference on machine learning, PMLR, 2022, pp. 11906–11917.
- [31] ZHULIU LI, TIANCI SONG, JEONGSIK YONG, AND RUI KUANG, *Imputation of spatially-resolved transcriptomes by graph-regularized tensor completion*, PLoS computational biology, 17 (2021), p. e1008218.
- [32] JI LIU, PRZEMYSŁAW MUSIAŁSKI, PETER WONKA, AND JIEPING YE, *Tensor completion for estimating missing values in visual data*, in 2009 IEEE 12th International Conference on Computer Vision, IEEE, 2009, pp. 2114–2121.
- [33] ———, *Tensor completion for estimating missing values in visual data*, IEEE transactions on pattern analysis and machine intelligence, 35 (2012), pp. 208–220.
- [34] YUANYUAN LIU, FANHUA SHANG, LICHENG JIAO, JAMES CHENG, AND HONG CHENG, *Trace norm regularized CANDECOMP/PARAFAC decomposition with missing data*, IEEE transactions on cybernetics, 45 (2014), pp. 2437–2448.
- [35] RAHUL MAZUMDER, TREVOR HASTIE, HASTIE@STANFORD EDU, ROBERT TIBSHIRANI, TIBS@STANFORD EDU, AND TOMMI JAAKKOLA, *Spectral Regularization Algorithms for Learning Large Incomplete Matrices*, Journal of Machine Learning Research, 11 (2010), pp. 2287–2322.

- [36] BORIS S MORDUKHOVICH, *Variational analysis and generalized differentiation I: Basic theory*, vol. 330, Springer Science & Business Media, 2006.
- [37] MORTEN MØRUP, LARS KAI HANSEN, CHRISTOPH S HERRMANN, JOSEF PARNAS, AND SIDSE M ARNFRED, *Parallel factor analysis as an exploratory tool for wavelet transformed event-related eeg*, *NeuroImage*, 29 (2006), pp. 938–947.
- [38] ATSUHIRO NARITA, KOHEI HAYASHI, RYOTA TOMIOKA, AND HISASHI KASHIMA, *Tensor factorization using auxiliary information*, *Data Mining and Knowledge Discovery*, 25 (2012), pp. 298–324.
- [39] MADHAV NIMISHAKAVI, PRATIK KUMAR JAWANPURIA, AND BAMDEV MISHRA, *A dual framework for low-rank tensor completion*, in *Advances in Neural Information Processing Systems*, 2018, pp. 5489–5500.
- [40] JIAHAO PANG AND GENE CHEUNG, *Graph Laplacian regularization for image denoising: Analysis in the continuous domain*, *IEEE Transactions on Image Processing*, 26 (2017), pp. 1770–1785.
- [41] NATHANAËL PERRAUDIN, JOHAN PARATTE, DAVID SHUMAN, LIONEL MARTIN, VASSILIS KALOFOLIAS, PIERRE VANDERGHEYNST, AND DAVID K HAMMOND, *GSPBOX: A toolbox for signal processing on graphs*, arXiv preprint arXiv:1408.5781, (2014).
- [42] NIKHIL RAO, HSIANG-FU YU, PRADEEP K RAVIKUMAR, AND INDERJIT S DHILLON, *Collaborative filtering with graph information: Consistency and scalable methods*, in *Advances in neural information processing systems*, 2015, pp. 2107–2115.
- [43] HOLGER RAUHUT, REINHOLD SCHNEIDER, AND ŽELJKA STOJANAC, *Tensor completion in hierarchical tensor representations*, in *Compressed Sensing and its Applications*, Springer, 2015, pp. 419–450.
- [44] BENJAMIN RECHT, MARYAM FAZEL, AND PABLO A PARRILO, *Guaranteed minimum-rank solutions of linear matrix equations via nuclear norm minimization*, *SIAM review*, 52 (2010), pp. 471–501.
- [45] R TYRRELL ROCKAFELLAR AND ROGER J-B WETS, *Variational analysis*, vol. 317, Springer Science & Business Media, 2009.
- [46] DAVID I SHUMAN, SUNIL K NARANG, PASCAL FROSSARD, ANTONIO ORTEGA, AND PIERRE VANDERGHEYNST, *The emerging field of signal processing on graphs: Extending high-dimensional data analysis to networks and other irregular domains*, *IEEE signal processing magazine*, 30 (2013), pp. 83–98.
- [47] NATHAN SREBRO, JASON RENNIE, AND TOMMI S JAASKOLA, *Maximum-margin matrix factorization*, in *Advances in neural information processing systems*, 2005, pp. 1329–1336.
- [48] NATHAN SREBRO AND RUSS R SALAKHUTDINOV, *Collaborative filtering in a non-uniform world: Learning with the weighted trace norm*, *Advances in neural information processing systems*, 23 (2010).
- [49] MICHAEL STEINLECHNER, *Riemannian optimization for high-dimensional tensor completion*, *SIAM Journal on Scientific Computing*, 38 (2016), pp. S461–S484.
- [50] GIORGIO TOMASI AND RASMUS BRO, *PARAFAC and missing values*, *Chemometrics and Intelligent Laboratory Systems*, 75 (2005), pp. 163–180.
- [51] WENQI WANG, VANEET AGGARWAL, AND SHUCHIN AERON, *Efficient low rank tensor ring completion*, in *Proceedings of the IEEE International Conference on Computer Vision*, 2017, pp. 5697–5705.
- [52] LIANG XIONG, XI CHEN, TZU-KUO HUANG, JEFF SCHNEIDER, AND JAIME G CARBONELL, *Temporal collaborative filtering with bayesian probabilistic tensor factorization*, in *Proceedings of the 2010 SIAM international conference on data mining*, SIAM, 2010, pp. 211–222.
- [53] YANGYANG XU AND WOTAO YIN, *A block coordinate descent method for regularized multiconvex optimization with applications to nonnegative tensor factorization and completion*, *SIAM Journal on imaging sciences*, 6 (2013), pp. 1758–1789.
- [54] JIN ZENG, JIAHAO PANG, WENXIU SUN, AND GENE CHEUNG, *Deep graph Laplacian regularization for robust denoising of real images*, in *2019 IEEE/CVF Conference on Computer Vision and Pattern Recognition Workshops (CVPRW)*, 2019, pp. 1759–1768.
- [55] TENGFEI ZHOU, HUI QIAN, ZEBANG SHEN, CHAO ZHANG, AND CONGFU XU, *Tensor completion with side information: A Riemannian manifold approach*, in *Proceedings of the 26th International Joint Conference on Artificial Intelligence*, AAAI Press, 2017, pp. 3539–3545.
- [56] TINGHUI ZHOU, HANHUAI SHAN, ARINDAM BANERJEE, AND GUILLERMO SAPIRO, *Kernelized probabilistic matrix factorization: Exploiting graphs and side information*, in *Proceedings of the 2012 SIAM international Conference on Data mining*, SIAM, 2012, pp. 403–414.